

An atlas of mid-infrared spectra of galaxy nuclei

Patrick F. Roche,¹ David K. Aitken,² Craig H. Smith² and Martin J. Ward³

¹Department of Astrophysics, Oxford University, Keble Road, Oxford OX1 3RH

²Physics Department, University of New South Wales, ADFA, Campbell, ACT 2600, Australia

³Royal Greenwich Observatory, Madingley Road, Cambridge CB3 0EZ

Accepted 1990 September 10. Received 1990 September 5; in original form 1990 May 23

SUMMARY

The spectral energy distributions are presented for 60 galaxies for which 8–13 μm , and in some cases 17–23 μm , spectra have been obtained. These infrared (IR) bright galaxies are discussed in terms of their spectral properties in the mid-IR and the relationship with their far-IR properties. Almost all of the galaxies can be placed in one of three classes on the basis of their 8–13 μm spectra: those dominated by the family of narrow bands between 3–13 μm , those with featureless continua and those that display the silicate absorption band. H II region galaxy nuclei, i.e. those which contain powerful nuclear H II regions and whose mid-IR spectra are dominated by emission in the family of narrow emission bands display little dispersion in their IR properties. The equivalent width of the narrow emission bands, quantified by that of the 11.3- μm feature, the ratios of the intensity of the 11.3- μm feature to the [Ne II] fine-structure emission line and the *IRAS* 12–100 μm flux ratios vary little from object to object and a ‘generic’ 8–100 μm spectrum is proposed for the H II region nuclei. In contrast to the spectral uniformity of H II region nuclei, galaxies containing active nuclei have a marked range in spectral properties, from featureless mid-IR spectra to domination by deep silicate absorption bands, but with little evidence of the narrow emission features. The diversity in the 8–13 μm spectra of active galactic nuclei (AGN) is reflected in the dispersion of their far-IR properties. The silicate absorption band in AGN probably arises in dusty regions relatively close to the central source, but there is no detailed correspondence between the strength of the 10- μm silicate absorption and the far-IR emission. It is possible that the precise geometry of circumnuclear matter and the viewing angle from the Earth are important factors in determining the observed spectra of the active nuclei. The emission from H II region galaxies arises in extended diffuse regions where these factors are of less consequence. The region of the *IRAS* colour–colour diagrams that lies between the domains of the luminous AGN and the H II region galaxies may be populated by galaxies that contain both active nuclei and circumnuclear H II regions. However, the mid-IR spectra do not resemble simple mixtures of the signatures of these components, probably because of the influence of the AGN on the circumnuclear environment. The dramatic differences in the spectral signatures of the AGN and H II region nuclei imply that if starbursts are the precursors of AGN, the latter must become dominant on short time-scales.

1 INTRODUCTION

By combining the photometric data from the *IRAS* mission with ground-based observations at shorter wavelengths, it is possible to define the IR energy distributions of the various classes of galaxy. Such studies have been carried out by a number of authors (e.g. Edelson & Malkan 1986; Ward *et al.*

1987) and have defined the overall spectral energy distributions. These show considerable dispersion from object to object. The most luminous active nuclei with powerful non-thermal emission often have IR spectral energy distributions that connect smoothly with optical and radio observations, suggesting continuity of the emission mechanism. Lower-luminosity active nuclei show more evidence of an additional

component peaking in the infrared and are most naturally explained as arising from emission from dust grains. [Here we use the term active galactic nuclei (AGN) to describe those objects which have evidence of non-stellar, compact energy sources in their nuclei.] Galaxies with vigorous nuclear star formation also have strong thermal peaks in the infrared. Of course, normal spiral galaxies also emit substantially in the IR, where about half of their output emerges, with a large fraction being emitted by their galactic discs (see Becklin 1986; Miley & de Grijp 1986). There are many exceptions to this picture, but a general dependence of the spectral shape of the IR emission on galaxy classification has been established.

Spectroscopy in the infrared probes the details of the emission and may reveal spectral features arising from emission or absorption by dust, molecules or atomic species. The 8–13 μm window contains a number of different spectral features providing useful diagnostics of gas and dust, and many of these have been detected in galactic nuclei. Spectra of a number of galaxies in the 10- μm window have been published (e.g. Aitken & Roche 1985; Roche & Aitken 1985, and references therein), and the differences in the broad IR spectral energy distributions outlined above are reflected in the spectral properties between 8–13 μm .

There is a clear separation between the mid-IR spectral signatures of galaxies which have nuclei dominated by massive H II regions and those in which an active (e.g. Seyfert) nucleus resides; galaxies that have neither nuclear H II regions nor non-thermal activity are generally too faint or diffuse for spectroscopic measurements with existing instruments. The galaxies with powerful H II regions in their nuclei almost all show distinct spectral structure due to emission, and possibly absorption, by dust together with emission from collisionally excited ionic fine-structure lines. These galaxies, which have been termed starburst nuclei, are remarkably uniform in that some 90 per cent have infrared spectra dominated by emission in the family of narrow features between 3–13 μm , known as the unidentified infrared (UIR) bands and now generally attributed to emission by small grains or large molecules (see Leger, d'Hendecourt & Boccarra 1986). The presence of the bands between 8 and 13 μm , together with that at 3.3 μm (Moorwood 1986), provides direct evidence for the emission mechanism in the mid-IR. By contrast, the active nuclei have much less structured spectra which are often well fitted by approximately power-law distributions at these wavelengths, although silicate absorption bands are seen in some of the objects. Dust emission features are seen only rarely; where the narrow emission bands are detected, it is likely that they are produced by circum-nuclear H II regions rather than the active nucleus. A possible explanation of the difference in 8–13 μm spectra between the active and H II region nuclei, in terms of the destruction of small grains by the high-energy photon flux from the Seyfert nuclei, has been proposed by Aitken & Roche (1985). Models of the IR emission from galactic nuclei must account for these observations.

In this paper, we have constructed spectral energy distributions of a number of galaxies from the IRAS *Point Source Catalogue* fluxes and ground-based observations at shorter wavelengths. The purpose of this compilation is to investigate how the far-IR properties of the nuclei of galaxies vary as a function of different spectral signatures at 10 μm . We

present 8–13 μm , and in a few cases 17–23 μm , spectra of almost all the galaxy nuclei that have been studied spectroscopically at these wavelengths to date, and include new spectra of 20 objects. We investigate these energy distributions and see how the detailed shape of the 8–13 μm spectrum, and in particular the presence or absence of spectral features relates to other IR properties. We will demonstrate the surprising variety in the 10- μm properties and spectral energy distributions of active galaxies, which contrasts with the homogeneity of those nuclei dominated by H II region emission.

2 DATA

The energy distributions discussed here, and shown in Fig. 1, were produced by combining IRAS fluxes with 8–13 μm (and in a few cases 17–23 μm) spectrophotometry obtained with the UCL spectrometer and near-IR (1–5 μm) photometry mostly taken from the literature. This obviously forms a rather multifarious sample, but the main problem is that the near-IR photometry and the mid-IR spectroscopy were obtained on ground-based telescopes with relatively small (~ 5 arcsec) beams so that the energy distributions from 1–20 μm are representative of the nuclear emission. The IRAS beams were about 1–2 arcmin in size, and cover a substantial fraction of the entire galaxy except in the very nearest objects. Furthermore, the effective beam sizes at 12 and 25 μm were smaller than those at 60 and 100 μm so that the IRAS colours may be distorted in nearby objects. In any case, because the fluxes from galaxy discs rise steeply with wavelength, the effect of the large IRAS beams will usually be to increase the 60 and 100 μm fluxes relative to those at shorter wavelengths. The different effective beam sizes present some problems in trying to disentangle the emission from the nuclear component from possible contributions from the disc of the host galaxy in the far-IR.

The objects under discussion are all bright at 10 μm and are generally the brightest examples of the various galaxy classes. Most were originally selected from published photometry [primarily from Rieke (1978) or Rieke & Lebofsky (1978)] showing that the 10- μm flux in a small beam is above the sensitivity limit of the UCL spectrometer in a couple of hours integration on a large telescope (i.e. ≥ 150 mJy). After the release of the IRAS survey, we also included a number of galaxies that were found to be bright at 12 μm , but had not previously been observed at 10 μm . In addition to spectra published in a series of papers (Aitken *et al.* 1982, 1985; Aitken, Roche & Phillips 1981; Roche & Aitken 1985; Roche *et al.* 1984, 1986; Phillips, Aitken & Roche 1984) we present a number of new spectra obtained at the 3.8-m UKIRT, 3.9-m AAT or the 5-m Hale telescope; a log of observations together with the optical classifications of the galaxies and quantities such as the distance and infrared luminosities (with $H_0 = 75 \text{ km s}^{-1} \text{ Mpc}^{-1}$), is given in Table 1. We have also included spectra between 17–23 μm of a number of the brighter galaxies taken at UKIRT in 1985 July or 1986 June and some near-IR photometry of IRAS galaxies obtained through the service facility of UKIRT.

The IRAS photometry is taken from the *Point Source Catalogue* for most objects; for some weak sources that were not included in the catalogue, we have used fluxes from the literature. The references for these, together with those for

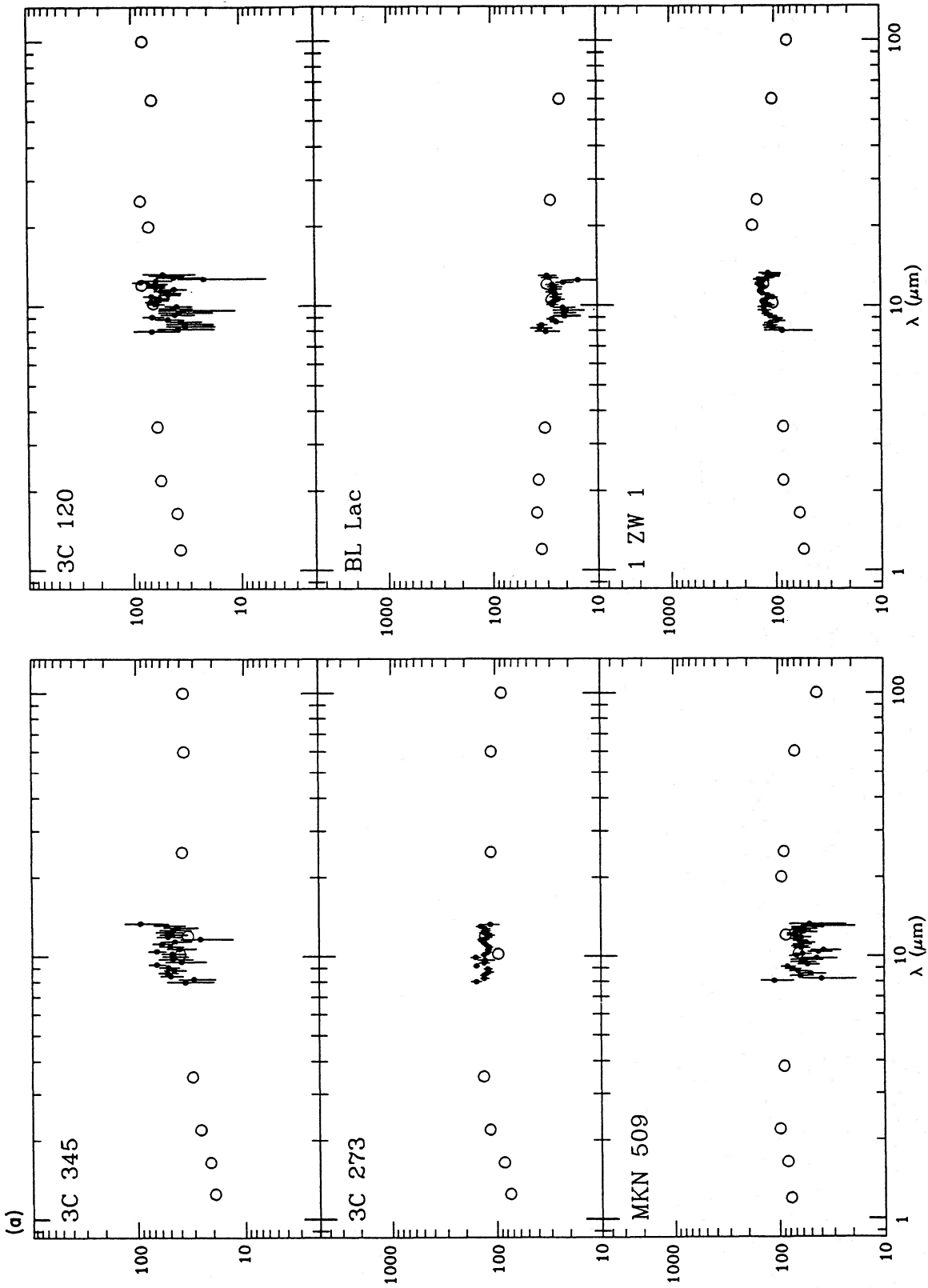


Figure 1. (a)–(k) The 1–100 μm spectral energy distributions of the galaxies in the sample (in units of $10^{-19} \text{ W cm}^{-2} \lambda F_{\lambda}$). The *IRAS* data are mostly from the *Point Source Catalogue* while the other photometry is from sources listed in Table 2. The galaxies are arranged in approximate order of increasing complexity in their 8–13 μm spectra, varying from galaxies with smooth featureless spectra through objects with silicate absorption minima to those dominated by prominent emission features. Included in Fig. 1(k) are ground-based and *IRAS* data on M82 showing that the shape of the mid-IR spectrum in the *IRAS* LRS beam is very similar to that measured from the ground in a 3-arcsec aperture (after allowing for the differences in resolution) despite a difference in flux of a factor of 30.

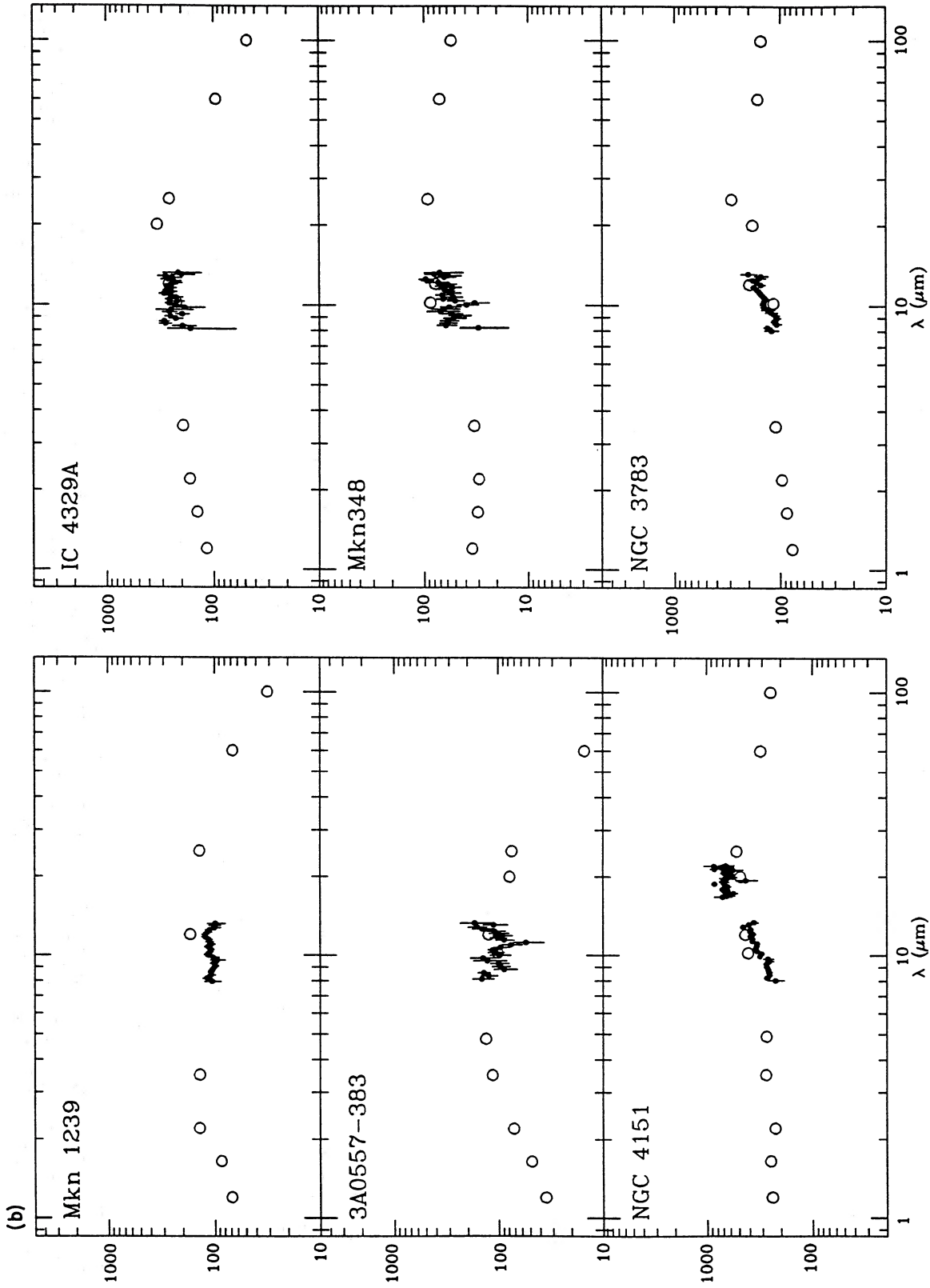


Figure 1 - continued

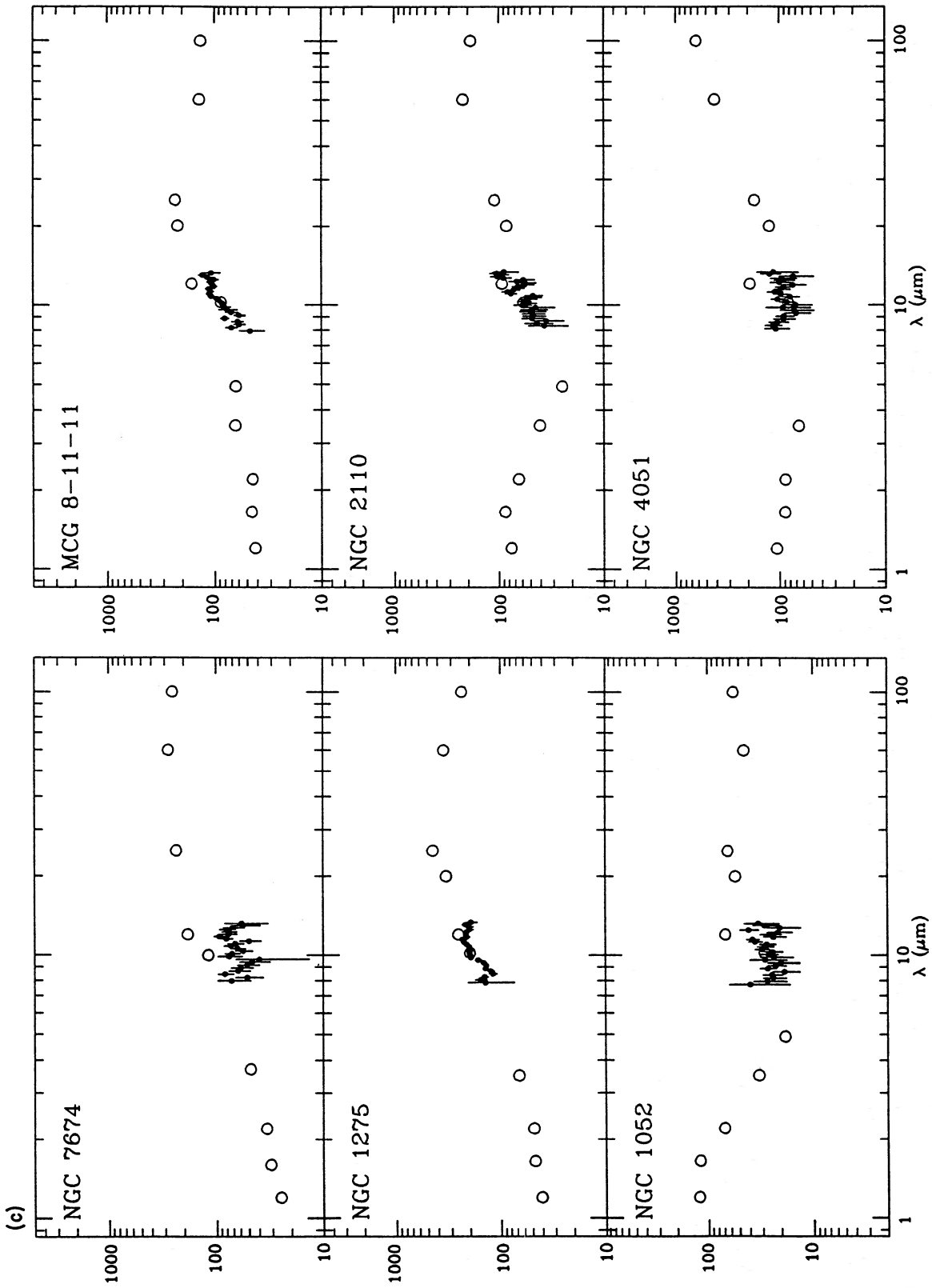


Figure 1 - continued

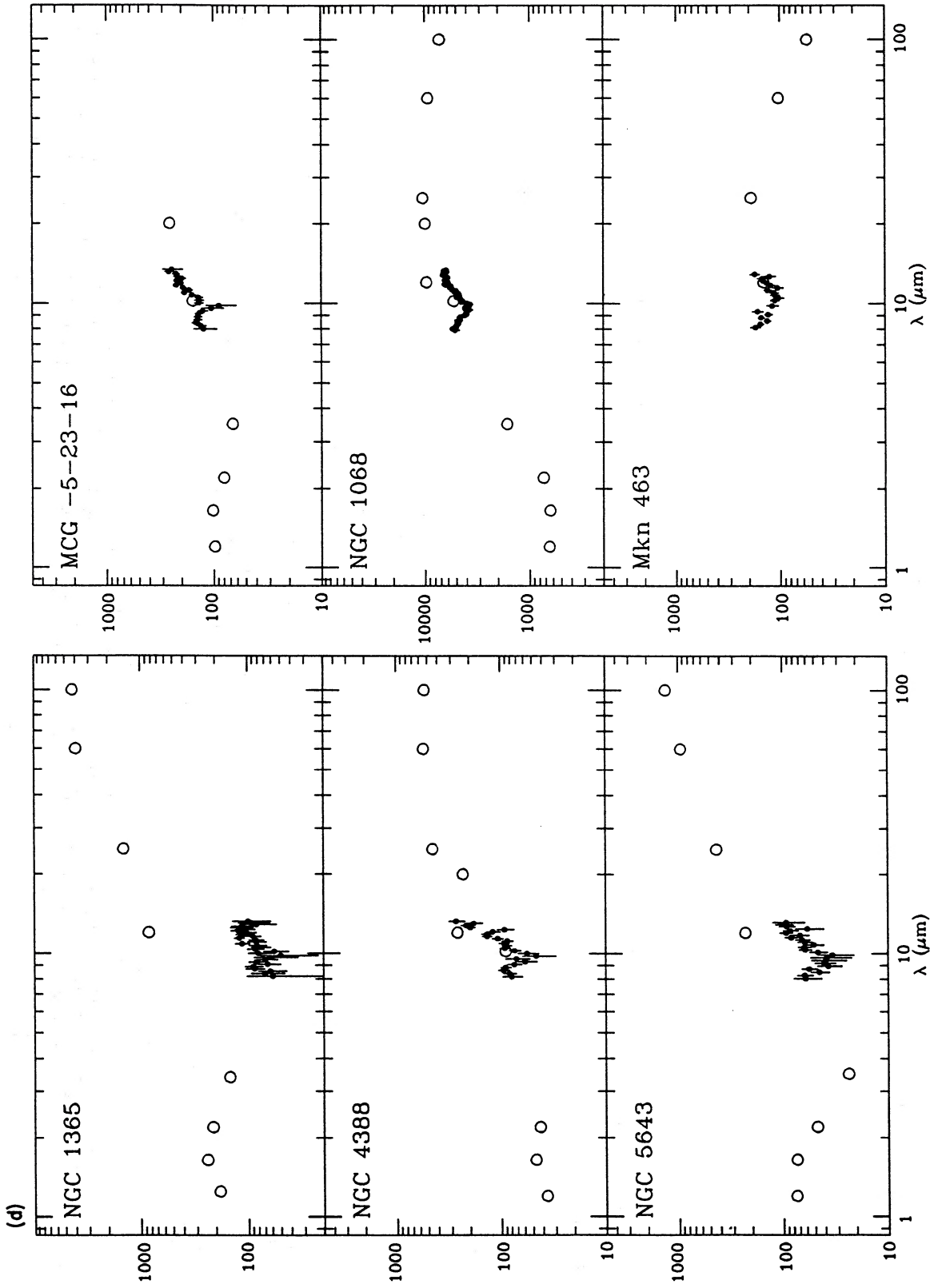


Figure 1 - continued

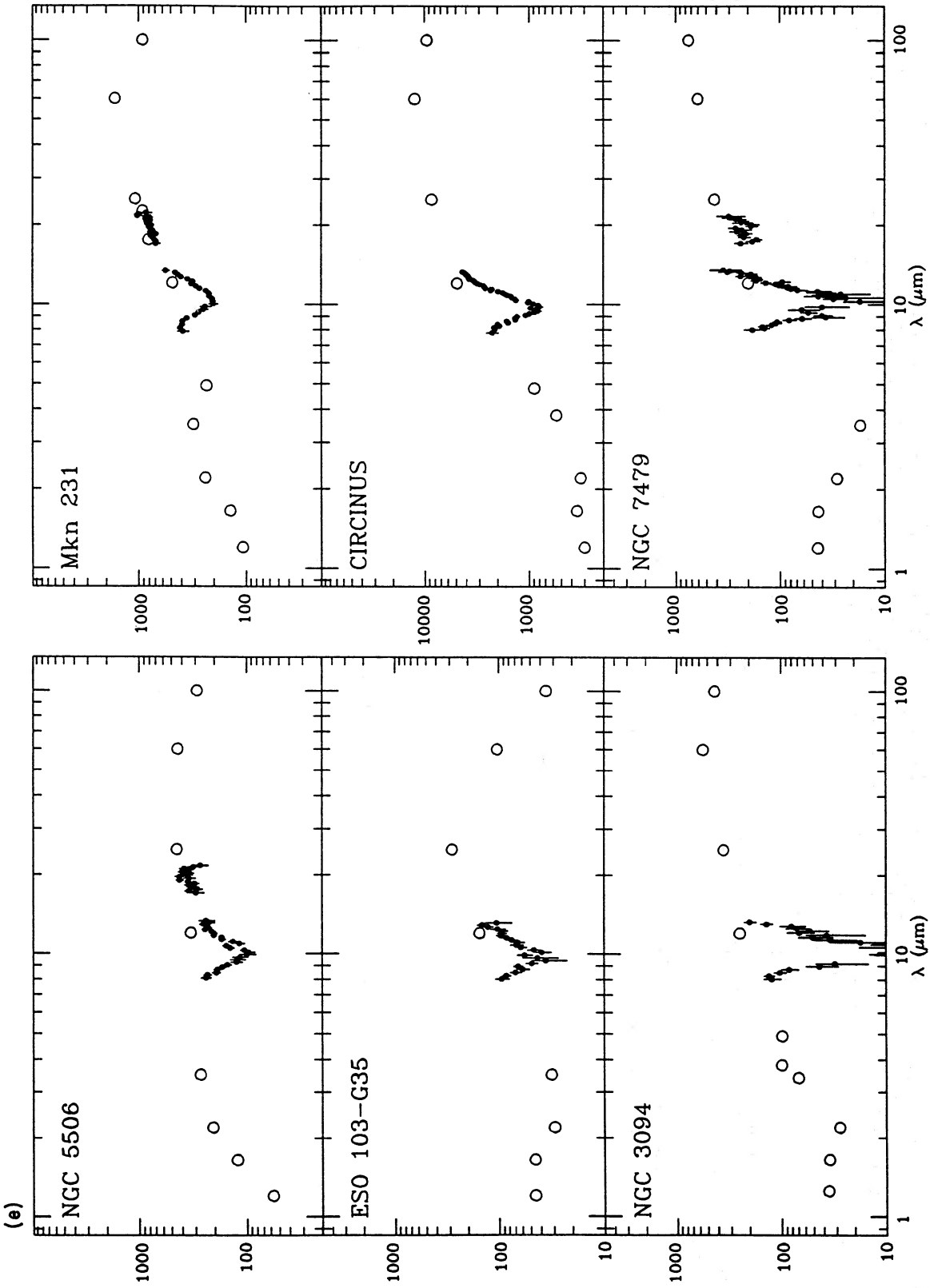


Figure 1 - continued

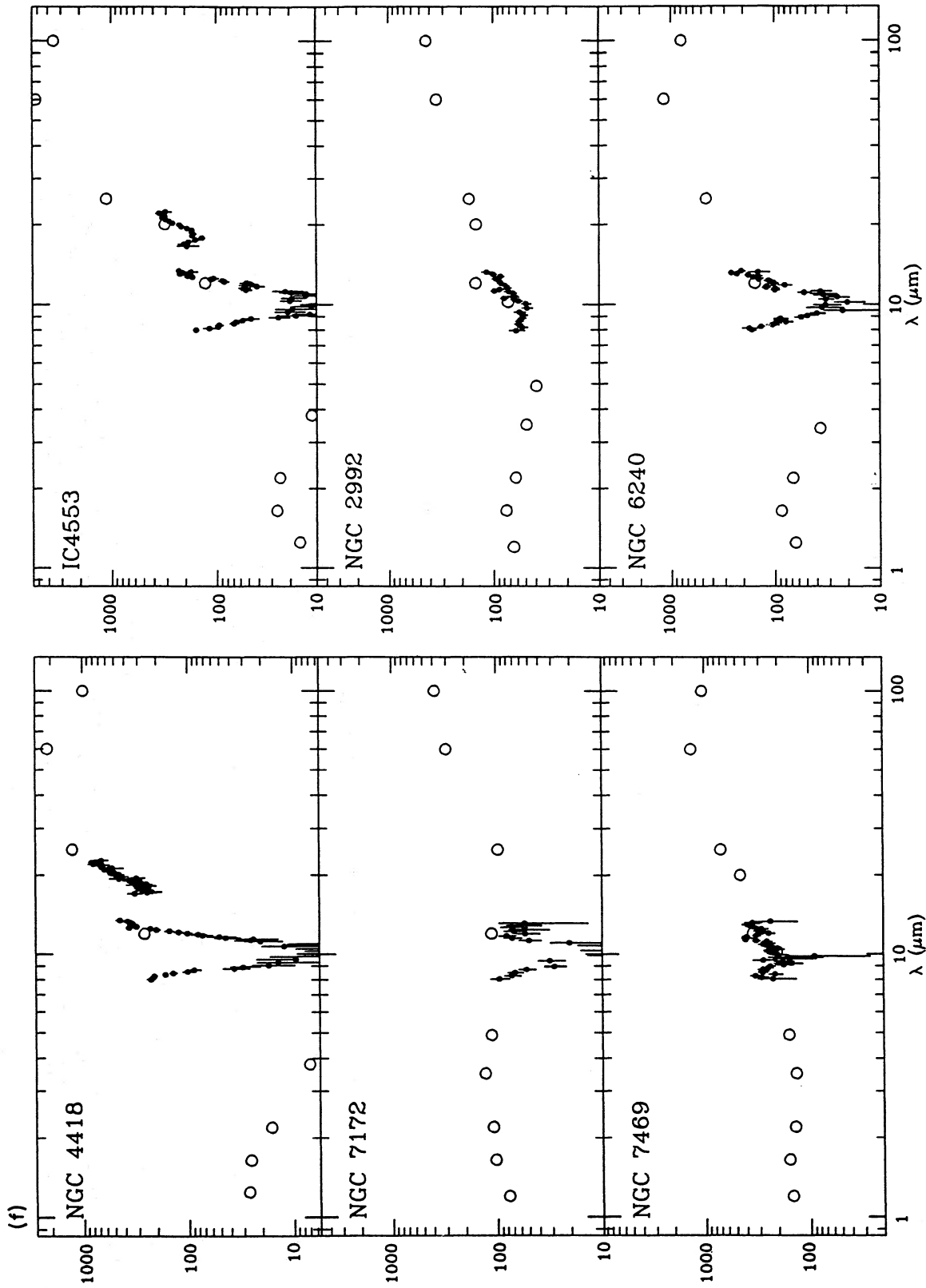


Figure 1 - continued

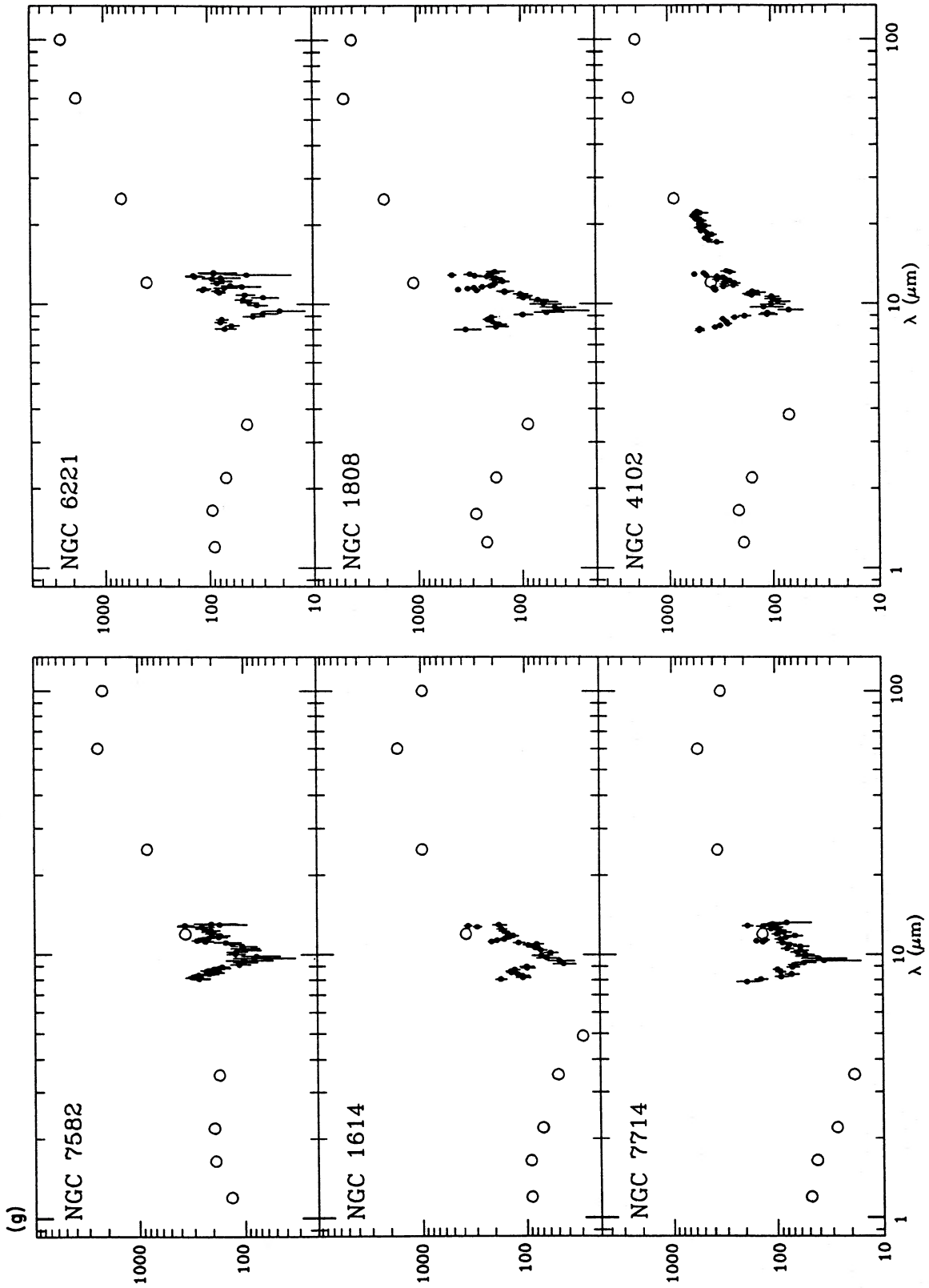


Figure 1 - continued

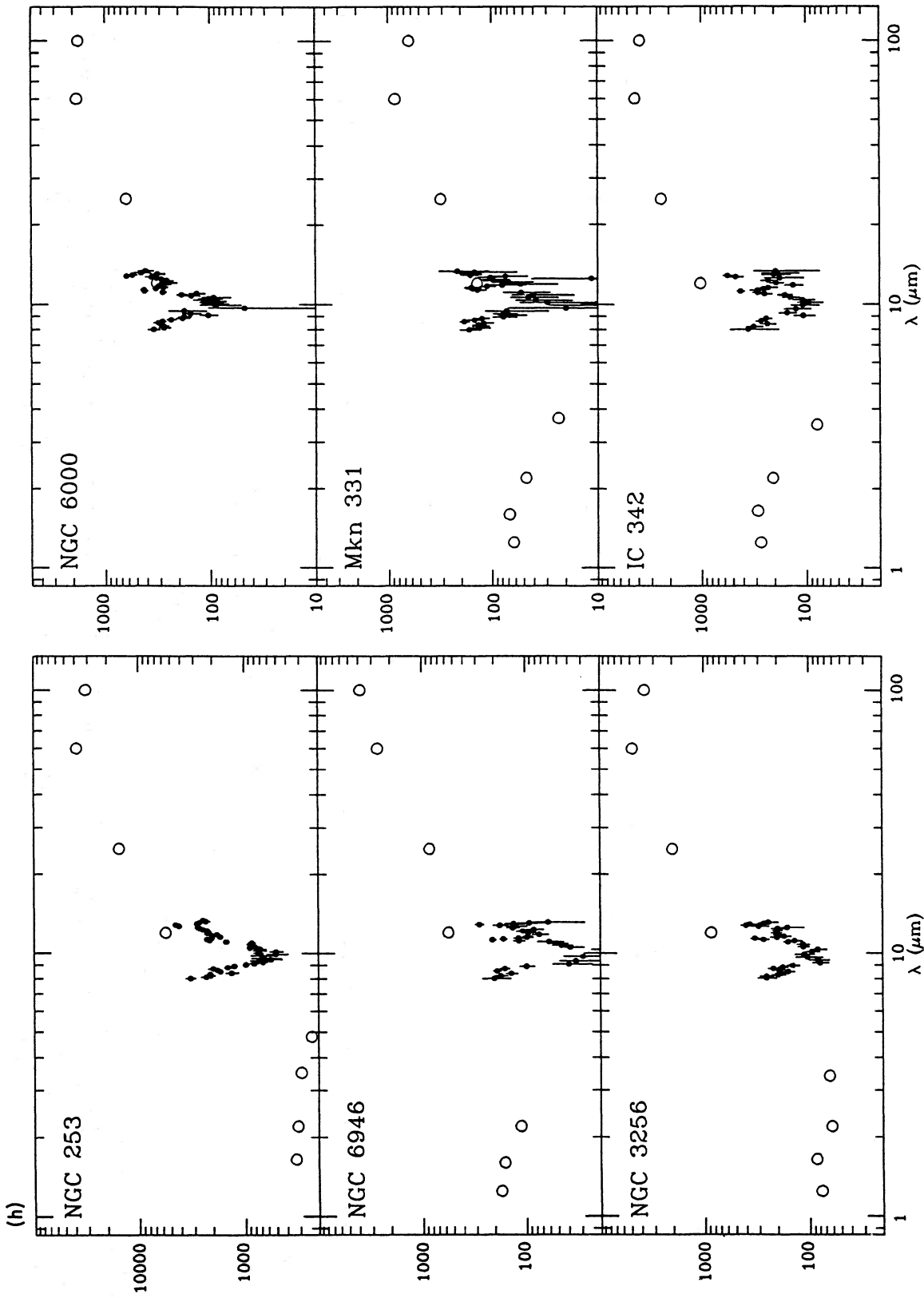


Figure 1 - continued

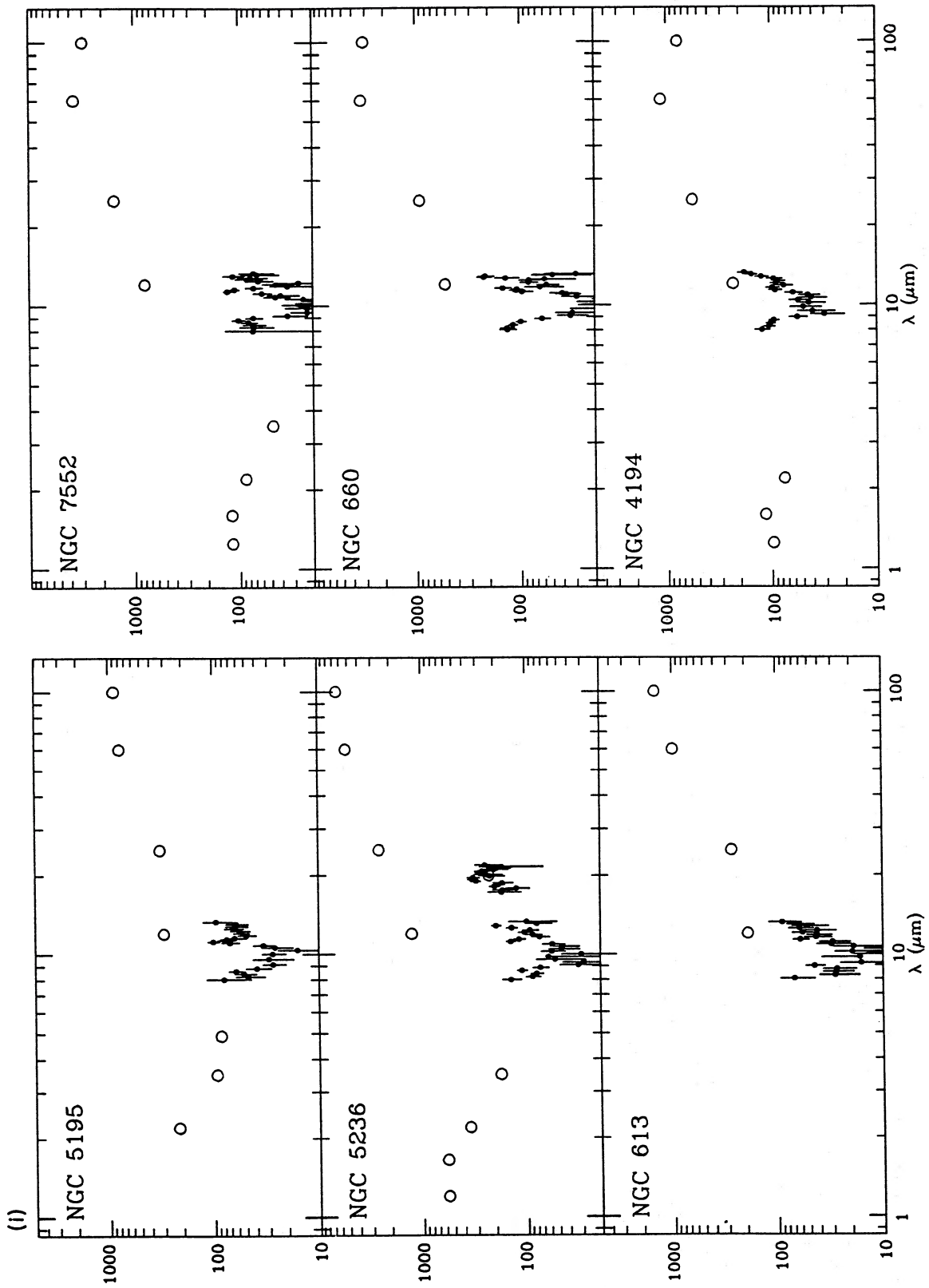


Figure 1 - continued

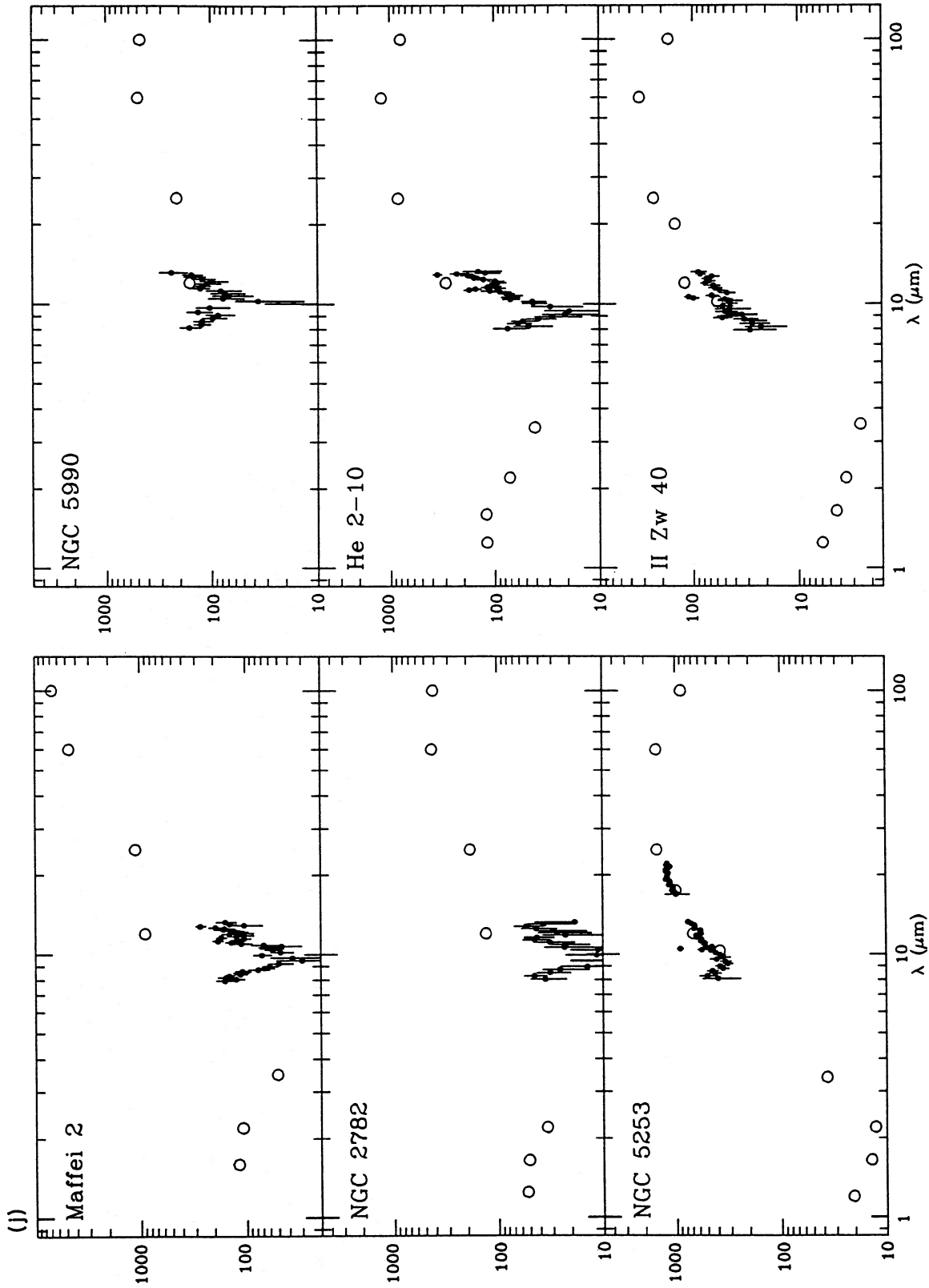


Figure 1 - continued

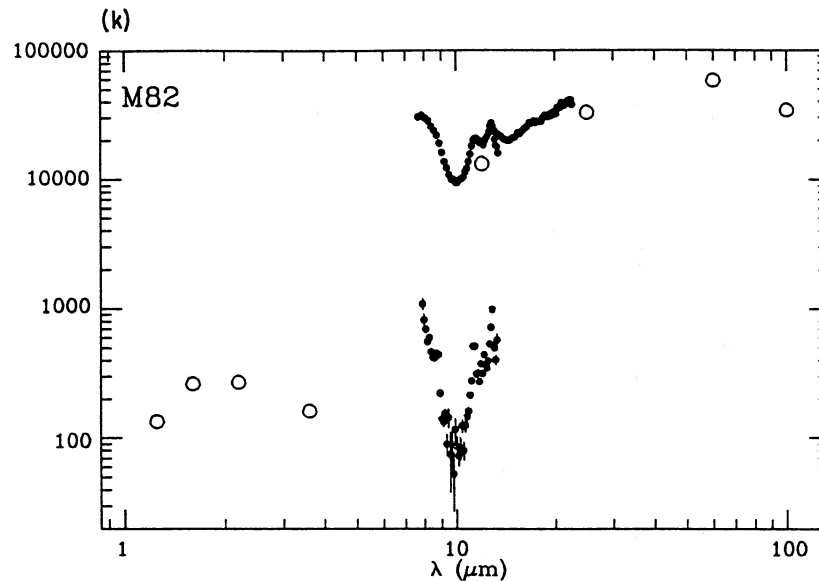


Figure 1 - continued

the ground-based photometry between 1 and 20 μm , are listed in column 13 of Table 2. Where a choice of photometry is available, which is quite often the case at *JHKL*, we have chosen the data that are closest to the aperture size used for the 8–13 μm spectra and nearest in time to the epoch of observations at 8–13 μm . Some of the objects are known to be variable in the IR, e.g. 3C 273, NGC 3783 and 3C 345 (Glass & Moorwood 1985; Robson *et al.* 1986; Bregman *et al.* 1986), and it is possible that some other active nuclei in which variability has not been proven also have significant variations in flux which could distort the spectral energy distributions presented here.

3 THE 1–100 μm ENERGY DISTRIBUTION

In Fig. 1 we have plotted the ground-based 1–20 μm photometry and mid-IR spectra together with the *IRAS* fluxes; the data and the sources of the measurements are listed in Table 2. Some assessment of the level of mid-IR emission arising from outside the nuclear region can be made by comparing the ground-based and *IRAS* fluxes at similar wavelengths. We have calculated 12- μm fluxes by averaging the 11–13 μm points in the 8–13 μm spectra and have listed the ratio of ground-based to *IRAS* fluxes in column 9 of Table 1.

It is clear that in almost all cases, the nuclear emission detected in the ground-based observations is less than that measured by *IRAS*, but that on average, nearly 50 per cent of the *IRAS* emission is contained within the small ground-based apertures. Caution must be exercised in interpreting these results. The galaxies were mostly selected on the basis of having high nuclear fluxes, and the observations were usually made at the peak of the visible emission so that the flux measured in a small beam would be reduced if the IR source is offset from the brightest optical peak. Further, some objects have complex spectral structure which renders colour corrections difficult.

In some galaxies a substantial amount of the 12- μm emission arises in regions more extended than a few hundred pc. A number of the galaxies in this sample are included in

the *IRAS* bright galaxy sample studied by Soifer *et al.* (1989), who have investigated the spatial extent of the IR emission measured by *IRAS* on scales of ~ 1 arcmin; these are indicated in Table 1. Interestingly, the median ratio of ground-based to *IRAS* 12- μm flux is the same for the galaxies which they found to be unresolved at 12 μm as those which were resolved. In this sample, the flag for whether the *IRAS* emission is extended is not a particularly good indicator of the ground-based to *IRAS* 12- μm flux ratio. However, selection effects are undoubtedly important, and the inclusion of galaxies that we did not detect with the spectrometer (see Section 5.4) would change this picture. The median values for the 12- μm flux ratios differ in the different classes of object, but the median distances also vary substantially (see Table 3). Extended star-formation regions are probably the dominant cause of these differences, but emission from the discs of the host galaxies may be important in some cases. (It is unlikely that variability accounts for the difference in more than one or two objects.)

4 THE RELATION BETWEEN 8–13 μm SPECTRA AND FAR-INFRARED FLUX

To investigate the relationship between the mid-IR spectra and the far-IR properties, we have divided the galaxies in this sample into three different classes, based on their 8–13 μm spectra:

- (i) objects with featureless 8–13 μm spectra;
- (ii) those that show clear silicate absorption at 10 μm ;
- (iii) those that show the 7.7-, 8.7- and 11.3- μm features.

In a sense, these divisions are provisional as higher-signal-to-noise spectra may reveal weak silicate absorption or weak emission from the family of emission features in galaxies that are apparently featureless, but at this point we are concerned with investigating the gross properties. The first and third groups are mutually exclusive, but some of the galaxies with strong UIR emission bands probably also suffer silicate absorption.

Table 1. Log of observations.

Name	Type	Telescope	Date	Beam (arcsec)	Distance (Mpc)	L_{FIR} (L_{\odot})	$L_{8-13\mu m}$ (L_{\odot})	$\frac{12_{ground}}{12_{IRAS}}$	Beam (kpc)	
3C 345	Q	F	UKIRT	1983 May	4.3	2400	7.5 E12	4.0 E12	1.32	50
3C 120	S1	F	UKIRT	1981 Oct	4.7	130	4.0 E10	1.2 E10	0.64	3.0
3C 273	Q	F	UKIRT	1982 June	4.7	630	1.3 E12	7.0 E11	1.08	14
BL Lac	B	F	Palomar	1983 Nov	3.6	280	2.8 E11	3.9 E10	1.11	4.9
Mkn 509	S1	F	UKIRT	1981 Oct	4.7	140	3.8 E10	1.8 E10	0.73	3.2
1 Zw 1	S1	F	UKIRT	1981 Oct	4.7	240	1.8 E11	1.0 E11	1.02	5.5
Mkn 1239	S1	F?	Palomar	1983 Nov	3.6	76	1.0 E10	8.6 E 9	0.60	1.3
IC 4329A	S1	F	AAT	1981 June	4.5	56	8.2 E 9	1.1 E10	1.05	1.2
A 0557-38	S1	F?	AAT	1985 Aug	4.2	135	1.5 E10	3.1 E10	0.80	2.7
Mkn 348	S2	F	UKIRT	1981 Oct	4.7	56	6.6 E 9	2.7 E 9	0.86	1.3
NGC 4151	S1	F	UKIRT	1982 June	4.3	12	1.4 E 9	6.7 E 8	0.89	0.25
NGC 3783	S1	F	AAT	1984 May	4.2	36	7.0 E 9	2.8 E 9	0.87	0.7
NGC 7674	S2	F	UKIRT	1982 June	4.3	116	1.1 E11	1.3 E10	0.42 U	2.4
MCG 8-11-11	S1	Se?	UKIRT	1983 Dec	4.3	80	2.8 E10	8.6 E 9	0.67	1.7
NGC 1275	S1	Se	Palomar	1983 Nov	3.6	68	4.7 E10	1.5 E10	0.77	1.2
NGC 2110	S2	F	UKIRT	1981 Oct	4.7	30	6.2 E 9	7.6 E 8	0.86	0.68
NGC 1052	L	F	Palomar	1983 Nov	3.6	20	6.4 E 8	1.5 E 8	0.44	0.35
NGC 4051	S1	S	UKIRT	1982 June	4.3	9	1.3 E 9	1.1 E 8	0.46 R	0.19
NGC 1365	S1	F	AAT	1981 Nov	4.5	24	7.7 E10	7.3 E 8	0.12	0.52
MCG -5-23-16	S2	S	UKIRT	1983 May	4.3	32		2.4 E 9		0.67
NGC 4388	S2	S	AAT	1984 May	4.2	14	3.5 E 9	2.7 E 8	0.48 R1	0.29
NGC 1068	S2	S	UKIRT	1981 Oct	4.7	12	4.0 E10	1.1 E10	0.62	0.27
NGC 5643	S2	S	AAT	1984 May	4.2	12	5.1 E 9	1.3 E 8	0.36	0.24
Mkn 463	S2	S	UKIRT	1986 June	4.2	200	1.1 E11	8.3 E10	0.81	4.1
NGC 5506	S2	S	UKIRT	1982 June	4.7	28	9.8 E 9	2.1 E 9	0.63 R	0.64
Mkn 231	S1	S	UKIRT	1982 June	4.5	170	1.3 E12	1.5 E11	0.65	3.7
ESO 103-G35	S1	S	AAT	1984 May	4.2	52	7.7 E 9	3.0 E 9	0.66	1.1
Circinus	S2	S	AAT	1984 May	4.2	3	3.3 E 9	2.6 E 8	0.61	0.06
NGC 3094		S	UKIRT	1985 May	3.8	31	1.6 E10	1.2 E 9	0.20 U	0.57
NGC 7479	L	S	AAT/UKIRT	1984/1986	4.3	32	2.2 E10	1.5 E 9	0.70 R	0.67
NGC 4418		S	UKIRT	1985 May	3.8	29	4.8 E10	8.4 E 8	0.47 U	0.52
IC 4553	S2	S,U	UKIRT	1986 July	5.6	76	8.7 E11	4.7 E 9	0.70	2.06
NGC 7172	L	S	AAT	1984 May	4.2	34	1.2 E10	7.4 E 8	0.54	0.69
NGC 2992	S1	S,U	UKIRT	1983 Dec	4.3	28	1.0 E10	7.8 E 8	0.57	0.58
NGC 7469	S1	U	UKIRT/AAT	1980/1984	4.7	67	1.8 E11	1.6 E10	0.94 R	1.5
NGC 6240	L/HII	U	UKIRT	1986 July	5.6	96	3.1 E11	1.1 E10	0.77	2.61
NGC 7582	S2	U	AAT	1981 Jul	4.5	21	3.3 E10	1.1 E 9	0.60	0.46
NGC 6221	L	U	AAT	1984 May	4.2	16	1.7 E10	2.2 E 8	0.18	0.33
NGC 1614	HII	U	UKIRT/AAT	1980/1984	4.7	60	1.6 E11	1.4 E10	0.45 U	1.37
NGC 1808	S/HII	U	UKIRT	1981 Oct	4.7	12	2.2 E10	3.2 E 8	0.17	0.27
NGC 7714	HII	U	IRTF	1981 Oct	5.9	37	2.1 E10	1.7 E 9	0.77 U	1.06
NGC 4102	L/HII	U	UKIRT	1985 May	3.8	12	1.1 E10	5.5 E 8	0.78 R1	0.22
NGC 253	L/HII	U	UH	1982 July	7.6	3.3	1.3 E10	2.6 E 8	0.44 R	0.12
NGC 6000	HII	U	UKIRT	1986 July	5.6	27	4.3 E10	2.5 E 9	1.08	0.73
NGC 6946	HII	U	IRTF	1981 Oct	5.9	11	2.5 E 9	1.7 E 8	0.21	0.31
Mkn 331	HII	U	UKIRT	1986 June	5.6	73	1.3 E11	6.5 E 9	0.70 R2	1.99
NGC 3256	HII	U	AAT	1984 May	4.2	35	1.8 E11	1.4 E 9	0.25	0.71
IC 342	HII	U	UH	1982 July	7.6	4.5	2.7 E 9	6.5 E 7	0.26	0.17
NGC 5195	HII	U	UKIRT	1982 July	4.3	8	8.0 E 8	4.6 E 7	0.30 U	0.17
NGC 7552	HII	U	AAT	1981 Nov	4.5	20	4.4 E10	3.5 E 8	0.09	0.44
NGC 5236	HII	U	UKIRT	1983 May	4.3	7	1.0 E10	5.6 E 7	0.09	0.15
NGC 660	HII	U	AAT	1984 Sep	4.2	19	3.8 E10	4.4 E 8	0.19 R	0.39
NGC 613	HII/S?	U	AAT	1984 Sep	4.2	19	1.5 E10	2.3 E 8	0.28 R	0.39
NGC 4194	HII	U	UKIRT	1985 May	3.8	36	4.2 E10	1.5 E 9	0.37	0.66
Maffei 2	HII	U	UKIRT	1989 Oct	4.2	5	3.6 E 9	3.7 E 7	0.16	0.10
NGC 5990	HII	U	UKIRT	1986 June	5.6	51	4.0 E10	4.0 E 9	0.71 U	1.39
NGC 2782	HII	U	UKIRT	1985 May	3.8	34	1.6 E10	5.3 E 8	0.27 R1	0.63
He 2-10	HII	U	IRTF	1981 Oct	5.9	8	2.2 E 9	7.4 E 7	0.47	0.23
NGC 5253	HII	S	AAT	1981 March	5.4	4	6.8 E 8	1.2 E 8	0.91	0.10
II Zw 40	HII	F	Palomar	1983 Nov	3.6	10	8.8 E 8	9.0 E 7	0.56	0.18
M82	HII	U	Palomar	1983 Nov	3.6	3	1.7 E10	4.2 E 7	0.03	0.05

Notes. Column 2, optical classification: Q – quasar, B – BL Lac, S1 – Seyfert 1, S2 – Seyfert 2, L – Liner, HII – HII region nucleus. Column 3, dominant 8–13 μm spectral characteristic: F – featureless, S – silicate absorption, Se – silicate emission, U – UIR band emission. Column 6, spectrometer aperture used. Column 7, distance derived with $H_0 = 75 \text{ km s}^{-1} \text{ Mpc}^{-1}$. Column 8, far-infrared (60–100 μm) luminosity. Column 9, N-band luminosity contained within the spectrometer aperture. Column 10, ratio of ground-based to *IRAS* 12- μm flux. R indicates that Soifer *et al.* (1989) have determined that the galaxy was resolved by *IRAS*; where a number is given, this indicates which band is extended. U indicates that the emission was not resolved. Column 11, the spectrometer beam diameter at the adopted galaxy distance.

Table 2. Photometric fluxes (mJy).

Name	J	H	K	L	M	N	Q	12	25	60	100	Source
3C 345	8.0	11.7	19	36		136		136	318	727	1224	1.
3C 120	15	22	41	90		220	470	330	701	1315	2644	3.
3C 273	30.9	46.8	85	155		324	670	512	928	2198	2911	2.
BL Lac	13.9	21.2	27.1	37		90.5		120	230	450		23,24.
Mkn 509	31	45	72	113		220	470	342	736	1383	1412	5.
1 Zw 1	22	33	63	110		360	1100	522	1237	2127	2530	3,7.
Mkn 1239	27.5	47.5	102	161				680	1158	1344	1044	13.
IC 4329A	47	79	123	227		760	2240	1050	2163	1908	1587	5,8
3A0557-38	10	19.2	38	113	116	347	521	502	623	352	<370	8.
Mkn 348	14	17	22	39		300		315	773	1425	1832	3.
NGC 4151	97	138	167	325	449	1400	3230	1755	4386	6254	8350	7,10,23
NGC 3783	31	48	72	131		400	1240	792	2435	3305	5118	5,11.
NGC 7674	10.0	16.5	25	59		395		736	1960	5571	8478	28.
MCG 8-11-11	16.8	24.8	33	75	104	296	1470	651	1983	2768	4476	8.
NGC 1275	16.3	26	35	78		674	2230	1025	3730	7078	7925	9.
NGC 2110	30.6	48	48	47	41	198	562	373	918	4459	6261	6.
NGC 1052	49	66	51	38	30	97	359	270	530	890	1880	14.
NGC 4051	43	49	65	77		280	830	761	1441	8366	20940	3,7
NGC 1365	76	131	155	167				3345	11925	78930	141500	5.
MCG -5-23-16	39.2	56	59	79		530	1730					5,11.
NGC 4388	14.6	25.6	31			305	1537	1040	3740	10900	17790	5.
NGC 1068	260	350	540	1920		18000	66000	38300	86830	185800	240500	3,7.
NGC 5643	30	41	35	28				918	3590	18900	44190	5.
Mkn 463								578	1598	2080	1837	
NGC 5506	22.7	67.4	151	313		643	1670	1323	3716	8727	9620	5,8.
Mkn 231	43	77	175	360	380	1420		1929	8965	33260	30580	4.
ESO 103-G35	18	25	22	37				614	2357	2079	1177	5.
Circinus	121	195	240	701	1430	6000	17880	19580	71290	248700	315900	22.
NGC 3094	14.8	20	21	78		160		979	2922	11090	14270	21.
NGC 7479	17.7	24	21	20		263	1114	795	3492	12240	24930	20.
NGC 4418	11.1	14.2	11.9	9				1041	10520	43420	33120	21.
IC 4553	6.8	14.7	18.5	16			2090	516	9322	105200	117700	18,19.
NGC 7172	31	57	80	132	184			448	809	6018	12850	6.
NGC 2992	26.2	42	46	57	65	249	980	594	1422	6941	14440	8.
NGC 7469	58.9	87	102	159	259	690	3010	1379	5828	26950	35220	8,10
NGC 6240	27	48	50	42		260	1379	620	3810	23470	26550	5,16.
NGC 7582	53.5	104	142	201		877	2850	1436	6879	48500	72760	5,11.
NGC 6221	36.3	52	51	51		330		1555	5663	36690	84500	5.
NGC 1614	35.8	50	51	58	48	630	3100	1484	8119	33210	32060	6,7.
NGC 1808	92	149	131	103				4338	17060	98100	136500	5.
NGC 7714	19.3	23.3	20	22				534	3012	11230	11180	6.
NGC 4102	80.5	118	117	89				1542	7348	47850	68500	21.
NGC 253		180	230	340	370	2900	28000	22270	127300	764400	1045000	17.
NGC 6000								1286	5293	36940	59470	
NGC 6946	72	85	82			750	4700	2229	7015	52430	127900	7.
Mkn 331	26	36.4	34.9	29		273		557	2614	17150	20980	28.
NGC 3256	32	47	45	73				3422	16590	95580	121800	5.
IC 342	114	160	154	93				4075	20120	85550	127500	16.
NGC 5195			160	110	140	290		1200	2700	15700	19400	17,27.
NGC 7552	49.4	64	64	56				3171	12860	73670	100900	6.
NGC 5236	230	320	260	207		460	1500	4970	21030	104700	213800	5.
NGC 660								2095	7621	66050	103700	
NGC 613	79	114	100					757	2232	19770	49140	12.
NGC 4194	41	62	56					921	4685	22790	25940	12.
Maffei 2		63	79	60				3620	9240	93400	226600	25.
NGC 5990								639	1781	10038	15850	
NGC 2782	22	28	25					522	1544	8559	13810	12.
He 2-10	50	65	53	47				1188	7001	24080	26140	5.
NGC 5253	8.3	7.7	9.4	41		1300	6090	2730	12630	30630	29490	5,11.
II Zw 40	2.5	2.4	2.6	3		200		484	2006	6545	5756	15.
M82	56	141	200	195				53210	273980	1167700	1145100	26.

References: (1) Bregman *et al.* (1986); (2) Neugebauer *et al.* (1979); (3) Rieke (1978); (4) Rieke (1976); (5) Glass & Moorwood (1985); (6) Lawrence *et al.* (1985); (7) Lebofsky & Rieke (1979); (8) Ward *et al.* (1987); (9) Longmore *et al.* (1984); (10) McAlary *et al.* (1983); (11) Frogel, Elias & Philips (1982); (12) Balzano & Weedman (1981); (13) Rudy, LeVan & Rodriguez-Espinosa (1982); (14) Becklin, Tokunaga & Wynn-Williams (1982); (15) Wynn-Williams & Becklin (1986); (16) Depoy, Becklin & Wynn-Williams (1986); (17) Rieke & Low (1972); (18) Norris (1985); (19) Emerson *et al.* (1984); (20) Willner *et al.* (1985); (21) this work - UKIRT Service observations; (22) Moorwood & Glass (1984); (23) Edelson & Malkan (1987); (24) Gear *et al.* (1986); (25) Spinrad *et al.* (1973); (26) Rieke *et al.* (1980); (27) Soifer *et al.* (1989); (28) Carico *et al.* (1988).

Table 3. Median flux ratios and luminosities.

Type	$\frac{L_{12\mu\text{m}}(\text{ground})}{L_{12\mu\text{m}}(\text{IRAS})}$	Aperture (kpc)	$L_{12\mu\text{m}}(\text{IRAS}) (L_{\odot})$	$L_{\text{FIR}} (L_{\odot})$
Q/S1	0.80	1.5	3.6 E10	4 E10
S2/L	0.60	0.67	6 E9	1 E10
HII	0.28	0.31	2 E9	1.3 E10

We have examined the *IRAS* flux ratios as a function of 8–13 μm spectral properties and find that the tightest grouping is between the 12- and 60- μm (or 100- μm) ratio for the galaxies dominated by the UIR emission bands; the other objects show far more scatter (Fig. 2). Similarly the ratio of 25- μm flux with the other *IRAS* bands also shows a lot of scatter in the galaxies with no or weak UIR emission, suggesting that the relative prominence of the warm dust component identified in active nuclei by Miley & de Grijp (1986) varies considerably from source to source.

4.1 Galaxies with featureless 8–13 μm spectra

Many of the objects with featureless 10- μm spectra have 1–100 μm spectral distributions that are devoid of strong structure. The mid-IR spectra connect smoothly with near-IR photometry and *IRAS* data with spectral slopes $\alpha \approx -1$ between 1 and 100 μm (where $S_{\nu} \propto \nu^{\alpha}$). The flattest spectra are found in the most luminous objects, the radio-loud quasars 3C345 and 3C273, and it could be that non-thermal emission dominates (see Robson *et al.* 1986). However, in several sources weak structure near 3 μm , the so-called 3- μm bump (Neugebauer *et al.* 1979; Barvainis 1987), and/or a broad maximum with a peak near 25 μm is visible, suggesting emission from warm dust. It is quite possible that dust is an important component of the emission in all of these galaxies but accounting for a larger fraction of the mid-IR emission in radio-quiet objects. It is clear from inspection of the data in Fig. 1, that the slopes of the 8–13 μm spectra obtained from the ground follow the overall distributions found by *IRAS* in the mid-IR, although the 8–13 μm spectra are generally steeper than the 12–25 μm slope, suggesting that the detailed spectral distributions are not well represented by power-law functions (see Fig. 3).

The great majority of galaxies that fall within this category are Seyferts of type 1, with the two quasars and a few type 2 Seyferts or Liners completing the group. The absence of significant silicate absorption is consistent with this in the sense that the broad-line region in most of these objects is detected at visible wavelengths, suggesting that extinction by dust is small. Two of the nuclei, IC 4329A and especially 3A0557–383, have peculiar humped spectra showing a very broad smooth peak in the energy distribution in the mid-IR which falls off to both short and long wavelengths. It is interesting to note that these two Seyfert 1s both have very steep Balmer decrements (Wilson & Penston 1979; Fairall, McHardy & Pye 1982).

4.2 Galaxies whose spectra show silicate absorption at 9.7 μm

There is a considerable range in the depth of the silicate absorption feature towards the galaxy nuclei in this group. The energy distributions also cover a wider range than the

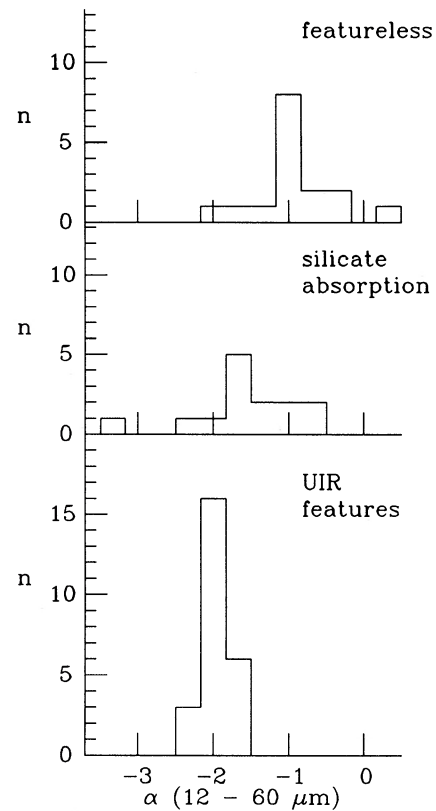


Figure 2. Histograms of the 12–60 μm spectral indices of galaxies with featureless 8–13 μm spectra, those with silicate absorption features and those dominated by UIR band emission.

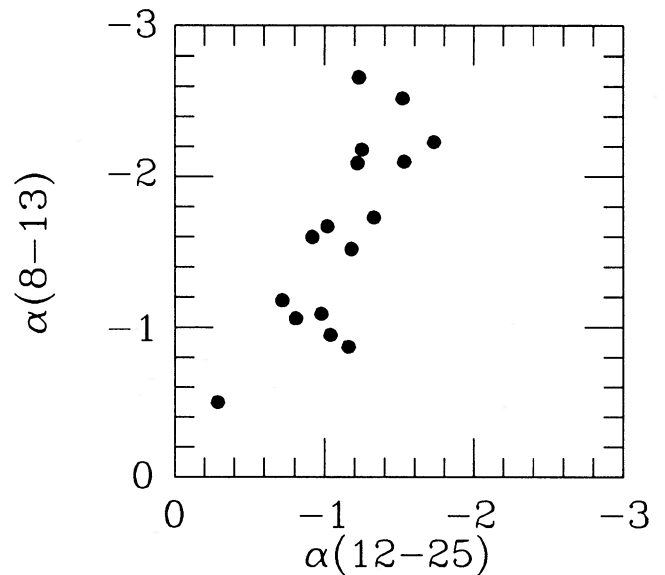


Figure 3. Spectral indices derived from the 8–13 μm spectra plotted against the 12–25 μm indices measured by *IRAS* for galaxies with featureless 8–13 μm spectra.

previous group. Most objects have steeply rising mid-infrared spectra, suggesting substantial thermal peaks in the far-IR, although some galaxies, e.g. ESO 103-G35, have a very prominent thermal component peaking near 30 μm .

Most of the galaxies with strong silicate absorption features that have been classified are classed as Seyferts of type 2, with a few peculiar objects such as Arp 220 and NGC 7479, together with peculiar Seyfert 1 galaxies such as Mkn 231 completing the group. The much larger fraction of S2 nuclei than S1 showing silicate absorption is consistent with the view that one of the principal differences between the two Seyfert classes is the opacity and covering factor around the nucleus (see Lawrence 1987). It is possible that some of the objects classed as type 2 Seyferts contain obscured type 1 nuclei in their cores, and indeed several of those for which this has been proposed, NGC 1068, NGC 4388, NGC 5506 and Mkn 463 (Antonucci & Miller 1985; Shields & Filippenko 1988; Blanco, Ward & Wright 1990; Hutchings & Neff 1989) are included in this compilation. Interestingly, these galaxies all show silicate absorption features, with $\tau_{9.7} = 0.52, 0.68, 1.31$ and 0.47 , respectively, indicating A_V between 5 and 20 mag, and account for half of the galaxies classed as Seyfert 2s with detectable $9.7\text{-}\mu\text{m}$ absorption. In general, the absorbing columns derived from the depth of the silicate absorption bands are in between those obtained from optical emission line ratios and the hydrogen columns inferred from soft X-ray cut-offs (Aitken & Roche 1985), but with no detailed correspondence between them. On the one hand, the hydrogen columns inferred towards ESO 103-G35 and NGC 7172, two galaxies with pronounced silicate absorption features, are two of the highest known, whilst on the other NGC 4151 shows no evidence of silicate absorption but has an X-ray cut-off that implies $A_V \approx 40$ mag (Turner & Pounds 1989). It is not clear whether the absorbing material producing the silicate feature is the same as that hiding the putative type 1 nuclei.

The galaxies with very pronounced silicate absorption bands must suffer large extinction towards their nuclei. In these cases, the visible spectra must emerge from relatively unobscured regions, implying low covering factors, or perhaps through scattering as suggested by polarization measurements for a few objects.

4.2.1 Silicate emission

Of the galaxies in our sample, only NGC 1275, and possibly MCG 8-11-11 shows direct evidence of silicate emission. These objects have $8\text{--}13\text{ }\mu\text{m}$ spectra that resemble the ‘Seyfert’ component adopted by Rowan-Robinson & Crawford (1989), but are not representative of most Seyfert nuclei. The general absence of silicate emission in our sample presumably reflects the small fraction of the luminosity arising from warm silicate grains; high-signal-to-noise $20\text{-}\mu\text{m}$ spectra could put further constraints on the emission from silicates. It is likely that Seyfert nuclei cover the entire range from silicate emission to absorption, and that these objects represent one extreme in the sample measured to date.

4.3 Galaxies with spectra dominated by the family of narrow emission bands

Virtually all of the galaxies that lie in this class are those with prominent H II regions in their nuclei. The spectra are dominated by emission peaks at $7.7, 8.7$ and $11.3\text{ }\mu\text{m}$,

usually accompanied by the $12.8\text{-}\mu\text{m}$ [Ne II] fine-structure line. All of these galaxies have strong peaks in their energy distributions in the far-IR, and although the detailed shape varies from object to object, both the $8\text{--}13\text{ }\mu\text{m}$ spectra and the IR energy distributions are similar to those of the archetypal starburst galaxies NGC 253 and M82 (Gillett *et al.* 1975). A few of these objects have been classified as Seyferts; NGC 7469 and NGC 7582 are Seyferts of types 1 and 2, respectively. However, there are clearly bright circumnuclear star-formation regions in these two galaxies (Cutri *et al.* 1984; Ward *et al.* 1980), and it seems certain that the mid- and far-IR emission from the H II regions dominates over the Seyfert component. The IR distributions, peaking between 60 and $100\text{ }\mu\text{m}$, are similar to H II regions in the Galaxy. Most H II region galaxy nuclei have very similar IR spectra, with a tighter correlation between the 12- and $100\text{-}\mu\text{m}$ IRAS fluxes than the classes considered previously. The similarity of the H II region galaxies contrasts markedly with the diversity of the active nuclei.

5 DISCUSSION

5.1 IRAS colours

Fig. 4(a) shows the $12:25:6\text{-}\mu\text{m}$ colour-colour diagram from the IRAS survey of the sample, with the galaxies identified by

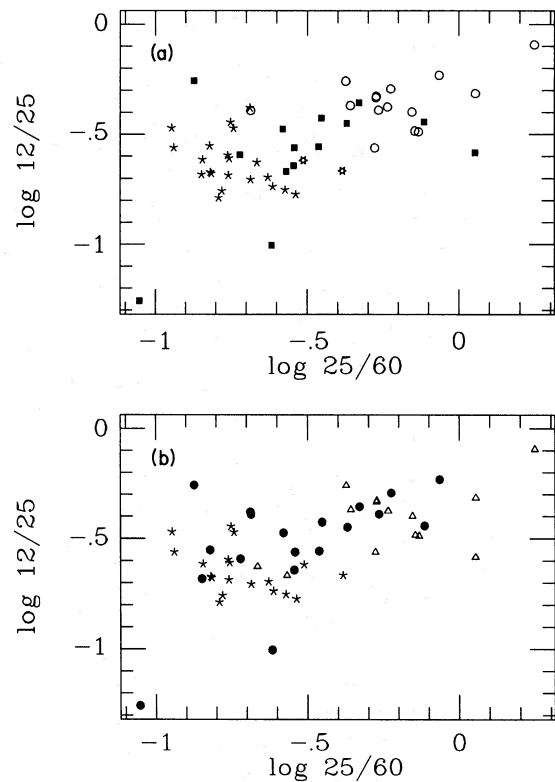


Figure 4. IRAS $12:25:60\text{-}\mu\text{m}$ colour-colour plots of the galaxies in our sample. (a) Classed according to their mid-IR characteristics: those with featureless $8\text{--}13\text{ }\mu\text{m}$ spectra are shown as open circles, galaxies with silicate absorption features as filled squares and those with UIR emission as stars. (b) According to their optical classifications: type 1 Seyferts and quasars are designated by open triangles, type 2 Seyferts by filled circles while H II region nuclei are represented by stars.

their 8–13 μm spectral characteristics. There is a clear separation between the galaxies with featureless 8–13 μm spectra and those dominated by the UIR bands. Nuclei with featureless spectra lie towards the top right of the plot (the ‘warm’ region) whilst those dominated by UIR band emission lie towards the bottom left. Apart from the most extreme examples, Arp 220, NGC 4418 and NGC 7172, the objects with silicate absorption lie between those with featureless spectra and those dominated by the UIR emission bands. In Fig. 4(b), the same plot is shown, but with the galaxies identified by classifications derived from their optical emission line properties. The domain of the objects dominated by UIR emission bands and those classed as H II region nuclei changes little in the two plots, but the differences in the other categories is much more marked. The different classes of galaxies are not as readily separable when optical classifications are used. This is not surprising as a classification based on spectral properties at 10 μm is likely to be directly relevant to the *IRAS* data and silicate absorption reduces the 12- μm flux whilst re-emission by cool dust grains increases the flux at longer wavelengths.

It has been suggested (e.g. Rowan-Robinson & Crawford 1989) that the objects populating the area of the diagram between the region of featureless spectra and those dominated by the UIR bands are composite objects with star-forming regions around an active nucleus. However, this region of the colour–colour diagram is populated by galaxies whose nuclei have 8–13 μm spectra which indicate that the mid-IR properties of the nuclear sources are different from those of both ‘pure’ AGN and H II region nuclei and do not look like a simple combination of the two. The spectra show silicate absorption features, but with no evidence of either UIR emission or fine-structure line emission. The fact that none of the fine-structure lines that fall within the 8–13 μm region have been detected in any of the nuclei occupying this part of the colour–colour diagram argues that not only the dust emission, but also the excitation conditions, are quite different from the H II region galaxies. In turn, this suggests that it is more likely that the silicate absorption features are intimately linked with the AGN themselves rather than circumnuclear H II regions, so that the 8–13 μm spectra of these objects do not provide supporting evidence for composite active/H II region nuclei.

It is possible that spectra with higher signal-to-noise than those presented here may reveal weak UIR emission features or fine-structure line emission from some of the objects in this region. Observation of the 3.3- μm band may be a more sensitive test of the presence of circumnuclear H II regions than the features in the 10- μm window. There would be no confusion from the silicate feature and the contribution to the continuum emission from dust is generally lower than at longer wavelengths. Alternatively, higher-resolution measurements of the fine-structure emission lines within the 8–13 μm window would provide better limits or more information on the excitation conditions in these objects.

Some galaxies clearly do show composite active/H II region nuclei. The Seyfert nucleus of NGC 1365 has a featureless spectrum, whilst the H II regions a few hundred parsec away have spectra dominated by UIR emission bands (Fig. 5), and it is probable that a spectrum taken in a large beam would be dominated by UIR emission. Similarly, NGC 7469 and 7582 contain Seyfert nuclei, but the

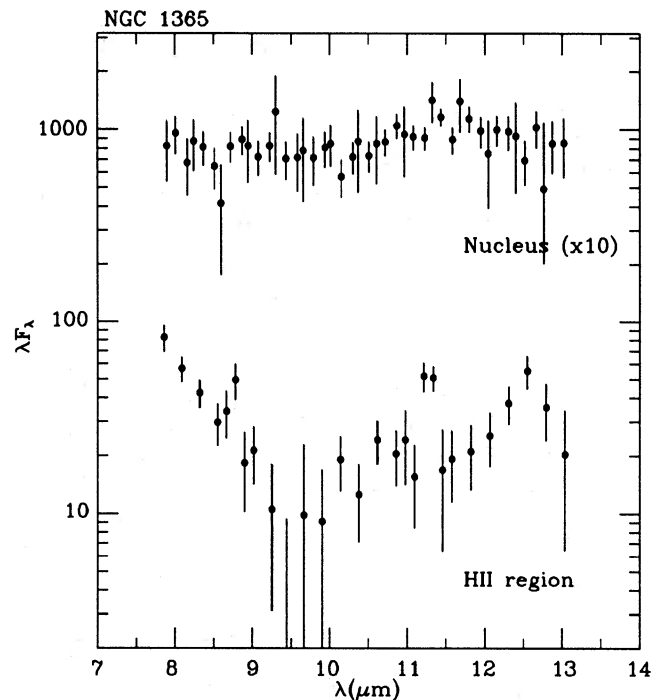


Figure 5. The 8–13 μm spectrum of the Seyfert nucleus of NGC 1365 compared to that of the bright optical H II regions lying ~ 800 pc to the south-west; both spectra were obtained in a 4.5-arcsec aperture.

emission from the central 5 arcsec is dominated by the UIR emission bands and so presumably by the circumnuclear H II regions; the spectra of the galaxies with silicate absorption features in Fig. 4(a) are quite distinct from these objects.

In view of the dramatic differences in IR properties between the H II region and AGN, we now discuss these groups separately.

5.2 H II region galaxies

5.2.1 Interpretation of the infrared spectrum

The presence of [Ne II] emission together with the non-detection of higher-excitation fine-structure lines that lie within the 10- μm window ([Ar III] at 9.0 μm and [S IV] at 10.5 μm) implies that the excitation of the gas is low, with effective temperatures of the exciting stars $\lesssim 35\,000$ K. The nuclear H II regions are not dominated by very hot or very massive stars, and better measurements or limits on the fine-structure line fluxes would be useful in further constraining the age or mass function of the stars.

We have calculated the equivalent width of the 11.3- μm feature and the [Ne II] emission line in the galaxies in our sample (Table 4). It is clear that the equivalent width of the 11.3- μm feature varies from object to object, but over quite a narrow range, with a mean of $0.34 \pm 0.17 \mu\text{m}$. The ratio of 11.3- μm feature flux to that in the [Ne II] line also does not vary dramatically from object to object, with a mean of 1.4 ± 0.7 , though there are a few objects in which the [Ne II] line was not detected and so could have higher ratios, and they have not been included in the calculated average. With some rather crude assumptions, we can use the [Ne II] line

flux as an estimate of the ionizing radiation emitted by the nuclear H II regions. These assumptions are that the abundance of neon is roughly solar, that, in view of the low excitation of the gas, neon is predominantly in the form of Ne⁺, and that the density in the ionized zone is below the critical density, i.e. $n_e \lesssim 10^5 \text{ cm}^{-3}$.

Following Rubin (1968), and adopting $T_e = 8000 \text{ K}$ and the collision strength for Ne⁺ from Seaton (1975), we can estimate the number of Lyman continuum photons

$$N_{\text{Lyc}} \sim 3.1 \times 10^{43} D^2 F[\text{Ne II}] \text{ photons s}^{-1},$$

where D is in Mpc and $F[\text{Ne II}]$ is in units of $10^{-20} \text{ W cm}^{-2}$.

The ratio of $11.3\text{-}\mu\text{m}/[\text{Ne II}]$ flux is then a measure of the power emitted in the UIR features compared to the number of ionizing photons for the volume contained within the spectrometer beam, and the small spread found for this ratio demonstrates that the UIR feature emission is closely related to N_{Lyc} , and hence the young star population in the H II region galaxy nuclei. We have argued that the emission features are produced primarily by absorption of non-ionizing photons escaping from the nuclear H II regions. At the low temperatures inferred for the exciting stars, most of the stellar flux is emitted at wavelengths longer than 912 \AA , and will escape from the H II region. In that case, the grains producing the narrow emission bands will be efficiently excited by the diffuse radiation and the emission will be proportional to the stellar luminosity. In turn, this will be proportional to the far-IR flux which is believed to reflect the total luminosity of the star-forming region.

What is perhaps surprising is that the detailed shape of the 8–13 μm spectrum in these H II region galaxy nuclei does not appear to depend on such quantities as the IR luminosity or

the axial ratio of the galaxy; the equivalent width of the $11.3\text{-}\mu\text{m}$ band or the ratio of $11.3\text{-}\mu\text{m}/[\text{Ne II}]$ emission show no clear dependence on other observable properties. Spectra taken at a number of positions within the central few hundred parsec of M82 differ somewhat in the relative strengths of the various features, but overall the variations are small (Jones & Rodriguez-Espinosa 1984). From this we can conclude that there is a typical 8–13 μm spectrum of H II region galaxy nuclei, covering a range in $10\text{-}\mu\text{m}$ luminosity from $< 10^8$ to $> 10^{10} L_{\odot}$. In turn, this suggests that the grain populations, especially the small carbon-rich particles proposed to explain the UIR bands (e.g. Duley & Williams 1981; Leger & Puget 1984), are not affected in any dramatic way by the nuclear H II regions. In particular, even the relatively violent events that accompany galaxy mergers which are believed to be occurring in, e.g. NGC 1614, 3256 and 6240 and which can produce large amounts of shocked gas (e.g. Joseph & Wright 1985), do not seem to lead to any great differences in the $10\text{-}\mu\text{m}$ spectra compared with galaxies having much less powerful nuclear star formation. This heightens the contrast with the Seyfert nuclei, where the UIR bands are seen very rarely, but the spectral properties vary considerably from object to object.

On the assumption that the $10\text{-}\mu\text{m}$ spectrum from the whole galaxy is similar to that measured in the small beams used for these observations, we can estimate the total emission from the UIR bands. When the other emission bands in the UIR family (i.e. those at 3.3 and $6.2 \mu\text{m}$, as well as the 7.7-, 8.6- and $11.3\text{-}\mu\text{m}$ features detected in these spectra are taken into account) about 1 per cent of the total luminosity of typical H II region galaxies emerges in the UIR bands.

Table 4. [Ne II] line and $11.3\text{-}\mu\text{m}$ feature intensities.

Galaxy	$F_{11.3}$	$F_{[\text{Ne II}]}$	$EW_{11.3}$	$\frac{F_{11.3}}{F_{[\text{Ne II}]}}$	N_{Lyc}
NGC 7469	45	96	0.19	0.47	1300
NGC 7582	36	20	0.27	1.80	27
NGC 1614	57	23	0.36	2.5	250
NGC 7714	15	7	0.25	2.1	30
NGC 3256	32	38	0.22	0.8	140
NGC 7552	27	< 10	0.70	> 2.7	<12
NGC 660	26	37	0.52	0.7	41
NGC 6221	17	10	0.37	1.7	8
NGC 1808	50	34	0.46	1.5	15
NGC 6946	22	15	0.49	1.5	6
He 2-10	12	20	0.22	0.6	4
NGC 5236	23	19	0.34	1.2	3
IC 342	85	64	0.61	1.1	4
NGC 253	310	330	0.24	0.9	11
M 82	2200	1930	0.16	1.1	95
NGC 6240	17	14	0.29	1.2	400
IC 4553	7	4:	0.23	1.7:	70
MKN 331	34	11:	0.70	3.0:	180
NGC 6000	61	41	0.31	1.5	90
NGC 4102	59	73	0.34	0.8	32
NGC 5990	12		0.15		
NGC 4194	12		0.20		
NGC 2782	11		0.54		
NGC 5195	20		0.55		
NGC 613	5		0.15		

Notes: line and feature intensities in units of $10^{-20} \text{ W cm}^{-2}$; Equivalent Width of the $11.3 \mu\text{m}$ feature in μm ; N_{Lyc} in units of 10^{52} photons s^{-1} .

5.2.2 A generic H II region galaxy spectrum

The narrow range of IR spectral properties exhibited by the H II region galaxies suggests that it may be possible to define a generic IR spectral energy distribution for these objects.

Most of the galaxies in this sample have sufficiently powerful star formation occurring in their nuclei that the far-IR output of the galaxies is probably dominated by the emission from the central few hundred parsec rather than the outer galaxy discs. In that case, the spectral shapes obtained through the relatively small apertures employed on ground-based telescopes will be representative of the total emission from the galaxies. In support of this view, we note that Puxley, Hawarden & Mountain (1988) found from radio studies that the enhanced star-formation activity in the *IRAS*-selected sample of nearby spirals is confined to the central regions, while Cohen & Volk (1989) found that the average spectrum of 20 galaxies culled from the *IRAS* Low Resolution Spectrometer database shows strong UIR emission.

We have derived a mean spectrum from the ground-based spectra and *IRAS* photometry of the H II region galaxies in our sample. The 8–100 μm energy distributions of the 12 brightest galaxies dominated by UIR emission (which have the highest quality 8–13 μm spectra) are shown in Fig. 6(a). They are normalized at $12 \mu\text{m}$ using the 11–13 μm flux for the spectra and the $12\text{-}\mu\text{m}$ photometry for the *IRAS* data. While there are small differences between the spectra, particularly in the 9–10 μm region where the silicate extinction peaks, the overall distributions are strikingly similar. Fig.

6(b) shows an estimate of the median spectrum of this sample of galaxies, which we propose defines the generic H II region galaxy nuclear component. This would seem an appropriate spectrum for use as the 'starburst' component in models of *IRAS* galaxies such as those constructed by Rowan-Robinson & Crawford (1989). The spectrum shown here is consistent with that produced by Cohen & Volk (1989), but the higher-resolution, higher-signal-to-noise spectra presented here show the spectral features much more clearly.

It is interesting to note that the histogram of 12/100 μm flux ratios of the IR bright objects in our H II region galaxy sample is very similar to that of all the galaxies in the *Revised Shapley Ames Catalogue* detected by *IRAS* in all four bands (Fig. 7), but with a higher fraction of 'warmer' galaxies. This may indicate that something like the 'generic' starburst galaxy spectrum is also present in the lower-luminosity normal galaxy population.

5.2.3 The high excitation nuclei of NGC 5253 and II Zw 40

Interestingly, the ratios of far-IR to mid-IR fluxes in the two starburst galaxies that do not show the narrow emission bands, the dwarf systems NGC 5253 and II Zw 40, are lower than those of the other H II region galaxies. These star-forming nuclei are of high excitation with strong [S IV] emission and with [Ne II] undetected, implying hot exciting stars and hence young starbursts. In this case, most of the stellar flux is emitted at wavelengths $< 912 \text{ \AA}$, and is trapped

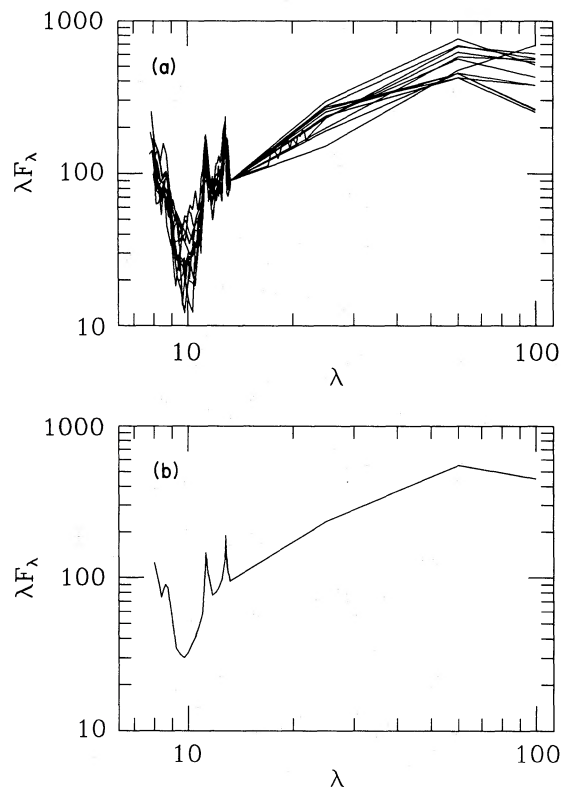


Figure 6. (a) Normalized 8–100 μm energy distributions of the 12 galaxies with spectra dominated by UIR emission and with the highest quality 8–13 μm spectra in the sample. (b) The average spectrum of this sample of galaxies, which provides the best estimate of a 'generic' nuclear H II region galaxy component. The 8–13 μm spectrum is at a resolution $\Delta\lambda \sim 0.24 \mu\text{m}$.

in the ionized region; these hard photons may destroy the particles that produce the UIR bands. However, it may be that 'normal-sized' grains in the ionized zone absorb a significant amount of the trapped radiation, and that the high-radiation field in that region produces a larger fraction of hot dust than can be found in the more typical H II region galaxies with lower excitation, thus giving higher 12- μm continua. II Zw 40 is certainly a metal-poor galaxy (Searle & Sargent 1972), whilst NGC 5253 appears to have approximately solar abundances of heavy elements (Osmer, Smith & Weedman 1979), implying that dust of a different mean composition from that in the other galaxies in the sample is unlikely to be the cause of the different 10- μm spectrum.

5.3 Active galaxies

In view of the large variations in the spectral properties of the AGN in this sample, it is clearly impossible to define a generic AGN spectrum. Part of the reason for this may be that the AGN spectra, particularly of the lower-luminosity objects, are contaminated by emission from other components of the host galaxies. In particular, circumnuclear star-formation regions could contribute, in which case the far-IR flux would be elevated with respect to the 10- μm flux. While this may be occurring in objects such NGC 5463 and 4051, many of the AGN actually emit less power at 100 μm than at

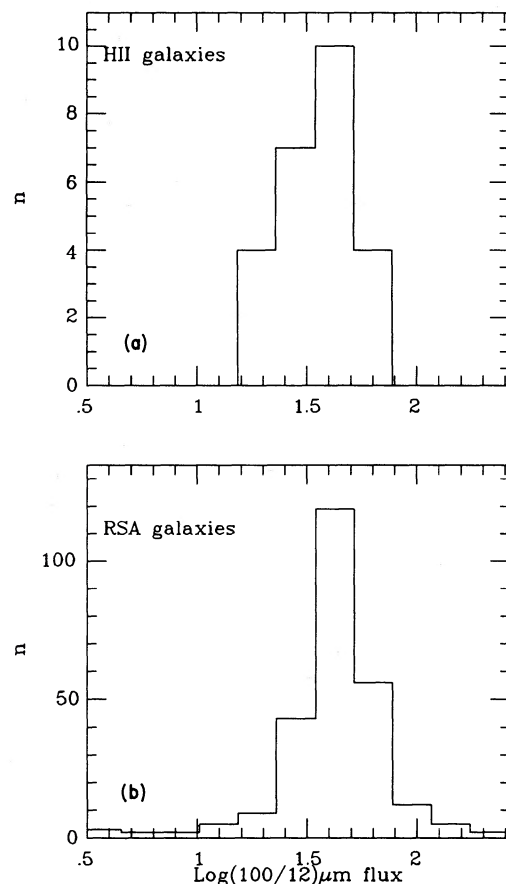


Figure 7. Histogram of the 100/12 μm flux ratio for (a) galaxies in our sample dominated by UIR emission at 8–13 μm , and (b) galaxies in the *Revised Shapley Ames Catalogue* detected by *IRAS* in all four bands.

10 μm . It appears that although it may be possible to model the AGN spectra as combinations of a featureless, non-thermal ‘power law’, a dust emission component and emission from stars, star-formation regions and the disc of the host galaxy, the dust emission component associated with the active nucleus must vary substantially from object to object.

Those galaxies that show evidence of a thermal peak in their *IRAS* data have steep 8–13 μm spectra, and it often appears (e.g. in the case of NGC 4151 or 3783) that the data at $\sim 8 \mu\text{m}$ lie close to a power law interpolated between the near-IR and 100- μm photometric data points, suggesting that the strong thermal peak only becomes visible at wavelengths longer than about 8 μm . In general, the spectral slope of the 8–13 μm nuclear spectrum is steeper than that given by the 12–25 μm *IRAS* measurements (Fig. 3), consistent with the view that the 8–13 μm spectra lie on the Wien side of the mid-IR thermal peak. Dust peaking at $\sim 20 \mu\text{m}$ has a characteristic temperature of $\sim 150 \text{ K}$, which is about the expected temperature of dust in the narrow-line regions of Seyfert nuclei (e.g. Kraemer & Harrington 1986).

Some objects are more extreme, ESO 103-G35 has a very prominent 25- μm bump whose 8- μm flux is much higher than an interpolation between the near-IR and 100- μm data. In this object the deep 9.7- μm silicate absorption feature implies that there must be a substantial optical depth at 10 μm towards the IR-emitting source. On the other hand, the fact that the IR-emission peak turns over near 25 μm and falls steeply to longer wavelengths demonstrates that most of the emission comes from dust warmer than $\sim 100 \text{ K}$. While it is possible that the 9.7- μm minimum arises through radiative transfer effects in optically thick clouds with temperature gradients close to the nucleus (see Kwan & Scoville 1976; Jones *et al.* 1977), it seems more likely that the dust resides in a disc-like geometry which intercepts only a fraction of the central luminosity, and where the observed silicate optical depth depends on the disc inclination to the line-of-sight. In the Kwan & Scoville models, the depth of the 10- μm minimum should be correlated with the mid- and far-IR colours, but for those Seyferts showing silicate absorption, there is little, if any, correlation of the silicate minimum with the 8–13 μm or the *IRAS* 25/60- or 60/100- μm colours; this statement holds true when the *IRAS*-selected galaxies are included from the next section. Thus, strong silicate absorption in these objects does not necessarily imply strong FIR emission.

The non-detection of the mid-IR fine-structure lines in AGN has been puzzling. Models of gas photo-ionized by Seyfert continua indicate that the [S IV] and/or [Ne II] lines should be quite bright in these objects with intensities brighter than or comparable to H β . For example, the model of Korista & Ferland (1989) predicts an [S IV] flux of $\sim 2.8 \times 10^{-19} \text{ W cm}^{-2}$ from NGC 4151, which is a factor of 3 higher than the 3σ limit from our spectrum. Oliva & Moorwood (1990) have detected the [Si VI] fine-structure line in NGC 1068 (with an intensity close to that predicted by Korista & Ferland), showing that very high-excitation conditions exist near the nucleus; it is possible that the non-detection of the mid-IR lines is due to densities significantly higher than those adopted in the models. It seems that in some objects, the active nucleus can have a profound influence on the surrounding material. We have argued that

the hard photon flux, which produces the high-excitation ionized gas, destroys the small grains or molecules believed to give rise to the UIR bands. This effect of the AGN on circumnuclear material could be responsible for the fact that the galaxies that populate the regions of the *IRAS* colour-colour diagrams between the AGN and H II region nuclei (discussed in Section 5.1) have mid-IR spectral properties which do not resemble a mixture of the two classes.

In summary, it appears that the details of the mid-IR emission from active nuclei depends, not only on the contributions from the host galaxy and the non-thermal source itself, but also on the detailed distribution of the dust clouds around the nucleus. Such quantities as the grain composition and the geometry and heating of the dust clouds obviously determine the emergent spectrum, but the viewing angle of observers on Earth may also be important, as there is good evidence that AGN are not spherically symmetric. Detailed modelling of the IR energy distribution and the mid-IR spectra of AGN may lead to useful constraints on the models.

5.4 *IRAS*-selected galaxies

One of the major fruits of the *IRAS* mission has been the discovery of a substantial number of galaxies that are extremely luminous in the infrared. The two most famed, and closest, examples are NGC 6240 and IC 4553 although several other objects were known to have extreme luminosities (e.g. Mkn 231, NGC 1614 and 3256 included in the present sample) before the *IRAS* results appeared. We have included a small number of galaxies detected by *IRAS* at 12 μm in this compilation. Several of these, such as NGC 6000 and 4102 have 10- μm spectra that are indistinguishable from the starburst nuclei discussed above. However, there are a number of objects that show deep 10- μm minima but show no evidence of strong emission in the UIR emission bands. In these objects, we interpret the spectral structure in the 8–13 μm window as being due predominantly to silicate absorption, implying a substantial column of cool dust along the line-of-sight to the emitting nuclei. In the most extreme of these galaxies, NGC 4418 (Roche *et al.* 1986), the optical depth at 10 μm is ~ 7 , corresponding to a visual extinction $A_V \sim 100 \text{ mag}$. Indeed the extinction is so high that even the near-IR colours show very little sign of the nuclear IR emission pinpointed by *IRAS*. Fig. 1 shows that in NGC 4418, the flux rises extremely steeply from 3.6 to 8 μm , and it is likely that the 1–4 μm photometry has detected stars in the nuclear bulge surrounding the IR source. NGC 3094 is a similar but less extreme object with a 10- μm optical depth of ~ 4.4 , but in this object the nuclear IR source is visible in the near-IR. Photometry shows that this galaxy has one of the reddest ($K-L$) colours of any galaxy, presumably resulting from a combination of reddening and the IR emission component detected at 10 μm . The 10- μm spectrum of NGC 7479, a galaxy classed as a Liner (Heckman, Balick & Crane 1980), is also less extreme than NGC 4418, but again shows little evidence of the mid- and far-IR source at wavelengths below 4 μm .

The spectra of IC 4553 and NGC 6240 have been discussed elsewhere (Smith, Aitken & Roche 1989). In the latter galaxy, there is clearly substantial emission in the 11.3-

μm feature, whilst in the former the 11.3- μm emission is weaker but still present. The presence of the UIR emission features renders it difficult to establish the depth of the 10- μm minimum due to silicate absorption, but, especially in IC 4553, the weakness of the 11.3- μm band compared to the depth of the 10- μm minimum implies that silicate absorption at 9.7 μm leads to a low flux in the *IRAS* 12- μm is the dominant process. Making allowance for the emission structure, it appears that there may be a nuclear source in IC 4553 with a silicate absorption depth comparable to that seen in NGC 4418, with a less heavily obscured region from which the UIR band emission originates. This could be an example of an obscured active nucleus with circumnuclear star formation.

Clearly, *IRAS* has identified a number of galaxies whose nuclear emission is heavily obscured at optical and sometimes even at near-IR wavelengths. In the most extreme examples, such as NGC 4418 and IC 4553, the deep silicate absorption at 9.7 μm leads to a low flux in the *IRAS* 12- μm band, rendering them easily selectable from their *IRAS* colours. Inspection of the galaxies with good *IRAS* fluxes in all four bands shows that these objects are quite rare, although, because the sensitivity of *IRAS* for the detection of galaxies was lowest in the 12- μm band, such objects would be selected against.

5.5 *IRAS*-selected galaxies not detected by us from the ground

For completeness, we mention the galaxies from the *IRAS Catalogued Galaxies* list which we observed briefly with the UCL spectrometer but did not find to be strong sources at 10 μm ; they are: NGC 134, 1084, 6574, 6835, 6921 and 7541. There are a number of possible reasons for this. We generally observed the peak of the optical emission with an aperture of about 4.5-arcsec diameter, so that any significant displacement between the optical and IR peak emission would reduce the 10- μm flux measured. The IR emission could be extended on a scale of ≥ 10 arcsec, so that only a small fraction of the *IRAS* 12- μm flux would be collected by the instrument. In general, the limit we can put on these galaxies is ≤ 100 mJy in our beam from summation of the 25 detectors in the spectrometer array. It is interesting that two of these objects, NGC 7541 and 6574, were observed by DePoy (1987) who failed to detect $\text{Br}\gamma$ or $\text{Br}\alpha$ in them; Deveraux (1987) gives 10- μm fluxes of 86 ± 19 and 82 ± 16 mJy for NGC 1084 and 7541, respectively, in a 5.5-arcsec beam.

6 RELATIONSHIP BETWEEN H II REGIONS AND ACTIVE NUCLEI

One of the unknown aspects of the nature of galaxies with luminous nuclei is the relationship between active nuclei and those with powerful H II regions. It has been suggested that large-scale star formation in the central regions of galaxies leads to the formation of the massive compact object that is supposed to lie at the heart of an active nucleus (Weedman 1983) – or vice versa. The collection of spectra assembled here does not readily lend support to such a progression unless the switch over is rapid and profoundly

affects either the nature of excitation of the dust grains in the central region.

In the case of the starburst galaxies, it appears that the dust composition is similar to that found in many regions of the galaxy, with evidence of contributions from silicate grains through the 9.7- and 18- μm absorption bands and from a population of the small carbon-rich dust particles that give rise to the family of UIR emission bands. The active nuclei also show evidence of silicates in many cases, but the UIR features are generally absent. There is evidence to suggest that Seyfert galaxies have higher element abundances than those found in starburst galaxies on average (e.g. Evans & Dopita 1987; Terlevich, Melnick & Moles 1987) which could affect the mix of different grain species in the different galaxies. However, it is unlikely that compositional differences of the dust on a galactic scale is responsible for the difference between the AGN and H II region nuclei as objects such as NGC 1365 and 7582 do show strong UIR emission from regions within a couple of hundred pc from the nucleus. It must therefore be concluded that it is the active nucleus itself that affects the dust emission process to suppress UIR emission, either by altering the grain composition within the nuclear region, perhaps by the selective destruction of grain species, or through very different excitation conditions.

The uniformity of H II region galaxy spectra may arise from emission from diffuse photodissociation zones mixed throughout a volume of 100 pc or more. In contrast, the active nuclei are probably dominated by one compact emitting source, so that geometric effects and viewing angles will have a much greater effect on the emergent spectrum. With greater understanding of the processes involved and high-spatial-resolution imaging, it may be possible to unravel some of the components.

7 CONCLUSIONS

(i) There appears to be a generic starburst spectrum for IR-bright galaxies with H II region nuclei over a broad range of luminosity, with prominent emission bands in the 3–13 μm region, ionic emission from low-excitation species and a relatively narrow range in 12/100- μm flux ratio, although differing amounts of silicate absorption cause variations in the depth of the minimum near 10 μm from galaxy to galaxy. The equivalent width of the 11.3- μm emission features lies within a narrow range, as does its ratio with the intensity of the 12.8- μm [Ne II] line indicating a strong correlation with the far-infrared luminosity. The 11.3- μm band probably provides a measure of the UV photons escaping from the ionized H II regions, while the [Ne II] line tracks the ionizing flux, so that the narrow spread in 11.3/12.8/100- μm flux ratios provides further evidence of a generic starburst galaxy spectrum.

The exceptions in this picture are the young low-luminosity starbursts in NGC 5253 and II Zw 40. These galaxies have emission lines of [S IV] at 10.5 μm (implying that the ionization is dominated by young hot stars), and do not show the UIR band emission. They also have higher 12/100- μm flux ratios indicating larger contributions from hot dust grains, presumably located within the H II regions.

(ii) With allowance for the intensities of the other emission bands in the UIR family, the 11.3- μm band flux implies that the luminosity emitted in the UIR bands is about

1 per cent of the total IR luminosity of these galaxies. The dust species responsible for the UIR bands must absorb at least this fraction of the short-wavelength radiation, and as they probably contribute significantly to the continuum emission, this fraction is very much a lower limit.

(iii) The galaxies with active (Seyfert) nuclei have very different 8–13 μm spectra from those dominated by H II regions, and also show a larger spread in *IRAS* colours. The UIR bands between 3 and 13 μm are seen only rarely, but the silicate absorption band is present in about half of the sample and is more prevalent in the lower-luminosity objects. There does not appear to be a generic AGN spectrum, but rather the emergent infrared spectrum probably depends upon the environment and geometry of the various components of the active nucleus.

(iv) Galaxies that display the various types of 8–13 μm spectrum lie in different parts of the 12:25:60- μm colour-colour diagram. This is well established for the division between H II region galaxies and AGN. However, the region between these two classes is populated by those AGN with silicate absorption features at 10 μm . These do not seem to be simply cases of AGN with circumnuclear H II regions, as neither the UIR bands nor the mid-IR fine-structure lines have been detected in these objects.

(v) Because large columns of silicate dust lie along the line-of-sight to the most heavily obscured nuclei, the 10- μm region is dominated by the silicate absorption band in these objects which depresses the 12- μm flux measured by *IRAS*. If a substantial fraction of the 12- μm flux is absorbed, there must be a high covering factor of obscuring material, and this is more likely to occur where the IR-emitting region is compact; selection of galaxies with low 12/25- μm fluxes will therefore preferentially select galaxies harbouring obscured AGN. A number of Seyfert 2s have silicate absorption yet similar *IRAS* colours to the Seyfert 1s, which have generally featureless spectra. This gives some support to the view that some, but perhaps not all, Seyfert 2s obscured Seyfert 1 nuclei.

(vi) Because of the remarkable separation in the mid-IR spectral properties, and to a lesser extent the *IRAS* photometric properties, of the different classes of galaxy, observations in the infrared can define, with a great deal of confidence, the dominant source of luminosity in the centre of galaxies.

ACKNOWLEDGMENTS

We are grateful for the assistance of the staff at the UKIRT, AAT, University of Hawaii, IRTF and Hale telescopes in ensuring that our observing runs were successful. We thank Tim Hawarden for helpful comments on the manuscript and acknowledge the support of the SERC and the ARGs.

REFERENCES

- Aitken, D. K. & Roche, P. F., 1983. *Mon. Not. R. astr. Soc.*, **202**, 1233.
- Aitken, D. K. & Roche, P. F., 1985. *Mon. Not. R. astr. Soc.*, **213**, 777.
- Aitken, D. K., Roche, P. F., Allen, M. C. & Phillips, M. M., 1982. *Mon. Not. R. astr. Soc.*, **199**, 31p.
- Aitken, D. K., Roche, P. F. & Phillips, M. M., 1981. *Mon. Not. R. astr. Soc.*, **196**, 101p.
- Aitken, D. K., Roche, P. F., Spenser, P. M. & Jones, B., 1979. *Astr. Astrophys.*, **76**, 60.
- Antonucci, R. J. & Miller, J. S., 1985. *Astrophys. J.*, **297**, 621.
- Balzano, V. A. & Weedman, D. W., 1981. *Astrophys. J.*, **243**, 756.
- Barvainis, R., 1987. *Astrophys. J.*, **320**, 537.
- Becklin, E. E., 1986. In: *Light on Dark Matter*, p. 415, ed. Israel, F. P., Reidel, Dordrecht.
- Becklin, E. E., Tokunaga, A. T. & Wynn-Williams, C. G., 1982. *Astrophys. J.*, **263**, 624.
- Becklin, E. E., Gatley, I., Matthews, K., Neugebauer, G., Sellgren, K., Werner, M. W. & Wynn-Williams, C. G., 1980. *Astrophys. J.*, **236**, 441.
- Blanco, P. R., Ward, M. J. & Wright, G. S., 1990. *Mon. Not. R. astr. Soc.*, **242**, 4p.
- Bregman, J. N. *et al.*, 1986. *Astrophys. J.*, **301**, 708.
- Carico, D. P., Sanders, D. B., Soifer, B. T., Elias, J. H., Matthews, K. & Neugebauer, G., 1988. *Astr. J.*, **95**, 356.
- Cohen, M. & Volk, K., 1989. *Astr. J.*, **98**, 1563.
- Cutri, R. M., Rudy, R. J., Rieke, G. H., Tokunaga, A. T. & Willner, S. P., 1984. *Astrophys. J.*, **290**, 521.
- DePoy, D. L., 1987. *PhD thesis*, University of Hawaii.
- DePoy, D. L., Becklin, E. E. & Wynn-Williams, C. G., 1986. *Astrophys. J.*, **307**, 116.
- Devereaux, N., 1987. *Astrophys. J.*, **323**, 91.
- Duley, W. W. & Williams, D. A., 1981. *Mon. Not. R. astr. Soc.*, **196**, 269.
- Edelson, R. & Malkan, M., 1986. *Astrophys. J.*, **308**, 59.
- Edelson, R. & Malkan, M., 1987. *Astrophys. J.*, **323**, 516.
- Evans, I. & Dopita, M., 1987. *Astrophys. J.*, **319**, 662.
- Fairall, A. P., McHardy, I. M. & Pye, J. P., 1982. *Mon. Not. R. astr. Soc.*, **198**, 13p.
- Frogel, J. A., Elias, J. H. & Phillips, M. M., 1982. *Astrophys. J.*, **260**, 70.
- Gear, W. K., Brown, L. M. J., Robson, E. I., Ade, P. A. R., Griffin, M. J., Smith, M. G., Nolt, I. G., Radostitz, J. V., Veeder, G. & Lebofsky, L., 1986. *Astrophys. J.*, **304**, 295.
- Gillett, F. C., Kleinmann, D. E., Wright, E. L. & Capps, R. W., 1975. *Astrophys. J.*, **198**, L65.
- Glass, I. S. & Moorwood, A. F., 1985. *Mon. Not. R. astr. Soc.*, **214**, 429.
- Heckman, T. M., Balick, B. & Crane, P. C., 1980. *Astr. Astrophys. Suppl.*, **40**, 295.
- Hutchings, J. B. & Neff, S. G., 1989. *Astr. J.*, **97**, 1306.
- Jones, B. & Rodriguez-Espinosa, J. M., 1984. *Astrophys. J.*, **285**, 580.
- Jones, T. W., Leung, C. M., Gould, R. J. & Stein, W. A., 1977. *Astrophys. J.*, **212**, 52.
- Joseph, R. D. & Wright, G. S., 1985. *Mon. Not. R. astr. Soc.*, **214**, 87.
- Korista, K. T. & Ferland, G. J., 1989. *Astrophys. J.*, **343**, 678.
- Kraemer, S. B. & Harrington, J. P., 1986. *Astrophys. J.*, **307**, 478.
- Kwan, J. & Scoville, N., 1976. *Astrophys. J.*, **209**, 102.
- Lawrence, A., 1987. *Publs astr. Soc. Pacif.*, **99**, 309.
- Lawrence, A., Ward, M., Elvis, M., Fabbiano, G., Willner, S. P., Carleton, N. P. & Longmore, A., 1985. *Astrophys. J.*, **291**, 117.
- Lebofsky, M. & Rieke, G. H., 1979. *Astrophys. J.*, **229**, 111.
- Leger, A. & Puget, J.-L., 1984. *Astr. Astrophys.*, **137**, L5.
- Leger, A., d'Hendecourt, L. & Boccarra, N., 1986. *Polycyclic Aromatic Hydrocarbons and Astrophysics*, Reidel, Dordrecht.
- Longmore, A. J., Sharples, R. M., Tokunaga, A. T., Rudy, R. J., Robson, E. I., Ade, P. A. R. & Radostitz, J., 1984. *Mon. Not. R. astr. Soc.*, **209**, 373.
- McAlary, C. W., McLaren, R. A., McGonegal, R. J. & Maza, J., 1983. *Astrophys. J. Suppl.*, **52**, 341.
- Miley, G. & de Grijp, R., 1986. In: *Light on Dark Matter*, p. 471, ed. Israel, F. P., Reidel, Dordrecht.
- Moorwood, A. F. M., 1986. *Astr. Astrophys.*, **166**, 4.

- Moorwood, A. F. M. & Glass, I. S., 1984. *Astr. Astrophys.*, **135**, 281.
- Neugebauer, G., Oke, J. B., Becklin, E. E. & Matthews, K., 1979. *Astrophys. J.*, **230**, 79.
- Neugebauer, G., Soifer, B. T., Rice, W. & Rowan-Robinson, M., 1984. *Publs astr. Soc. Pacif.*, **96**, 973.
- Norris, R. P., 1985. *Mon. Not. R. astr. Soc.*, **216**, 701.
- Oliva, E. & Moorwood, A. F. M., 1990. *Astrophys. J.*, **348**, L5.
- Osmer, P. S., Smith, M. G. & Weedman, D. W., 1979. *Astrophys. J.*, **192**, 279.
- Phillips, M. M., Aitken, D. K. & Roche, P. F., 1984. *Mon. Not. R. astr. Soc.*, **207**, 205.
- Puxley, P. J., Hawarden, T. G. & Mountain, C. M., 1988. *Mon. Not. R. astr. Soc.*, **231**, 465.
- Rieke, G. H., 1976. *Astrophys. J.*, **206**, L15.
- Rieke, G. H., 1978. *Astrophys. J.*, **226**, 550.
- Rieke, G. H. & Low, F. J., 1972. *Astrophys. J.*, **176**, L95.
- Rieke, G. H. & Lebofsky, M. J., 1978. *Astrophys. J.*, **220**, L37.
- Rieke, G. H., Lebofsky, M. J., Thompson, R. I., Low, F. J. & Tokunaga, A. T., 1980. *Astrophys. J.*, **238**, 24.
- Robson, E. I., Gear, W. K., Brown, L. M. J., Courvoisier, T. J.-L., Smith, M. G., Griffin, M. J. & Biecha, A., 1986. *Nature*, **323**, 134.
- Roche, P. F. & Aitken, D. K., 1984. *Mon. Not. R. astr. Soc.*, **208**, 481.
- Roche, P. F. & Aitken, D. K., 1985. *Mon. Not. R. astr. Soc.*, **213**, 789.
- Roche, P. F., Aitken, D. K., Phillips, M. M. & Whitmore, B., 1984. *Mon. Not. R. astr. Soc.*, **207**, 35.
- Roche, P. F., Aitken, D. K., Smith, C. H. & James, S. D., 1986. *Mon. Not. R. astr. Soc.*, **218**, 19p.
- Rowan-Robinson, M. & Crawford, J., 1989. *Mon. Not. R. astr. Soc.*, **238**, 523.
- Rubin, R. H., 1968. *Astrophys. J.*, **153**, 761.
- Rudy, R. J., LeVan, P. D. & Rodriguez-Espinosa, J. M., 1982. *Astr. J.*, **87**, 598.
- Seaton, M. J., 1975. *Mon. Not. R. astr. Soc.*, **170**, 476.
- Searle, L. & Sargent, W. L. W., 1972. *Astrophys. J.*, **173**, 25.
- Shields, J. C. & Filippenko, A. V., 1988. *Astrophys. J.*, **332**, L55.
- Smith, C. H., Aitken, D. K. & Roche, P. F., 1989. *Mon. Not. R. astr. Soc.*, **241**, 425.
- Soifer, B. T., Boehmer, L., Neugebauer, G. & Sanders, D. B., 1989. *Astr. J.*, **98**, 766.
- Spinrad, H., Bahcall, J., Becklin, E. E., Gunn, J. E., Kristian, J., Neugebauer, G., Sargent, W. L. W. & Smith, H., 1973. *Astrophys. J.*, **180**, 351.
- Terlevich, R., Melnick, J. & Moles, M., 1987. In: *Observational Evidence of Activity in Galaxies, IAU Symp. No. 121*, p. 499, eds Khachikian, E. Ye., Fricke, K. J. & Melnick, J., Reidel, Dordrecht.
- Turner, T. J. & Pounds, K. A., 1989. *Mon. Not. R. astr. Soc.*, **240**, 833.
- Ward, M. J., Penston, M. V., Blades, J. C. & Turtle, A. J., 1980. *Mon. Not. R. astr. Soc.*, **193**, 563.
- Ward, M., Elvis, M., Fabbiano, G., Carrleton, N. P., Willner, S. P. & Lawrence, A., 1987. *Astrophys. J.*, **315**, 74.
- Weedman, D. W., 1983. *Astrophys. J.*, **266**, 479.
- Willner, S. P., Elvis, M., Fabbiano, G., Lawrence, A. & Ward, M. J., 1985. *Astrophys. J.*, **299**, 443.
- Wilson, A. S. & Penston, M. V., 1979. *Astrophys. J.*, **232**, 389.
- Wynn-Williams, C. G. & Becklin, E. E., 1986. *Astrophys. J.*, **308**, 620.